Scanning Microscopy

Volume 3 | Number 3 Article 6

10-26-1989

Backscattered Electron Imaging Using Single Crystal Scintillator Detectors

R. Autrata
Czechoslovak Academy of Sciences

Scanning Microscopy, Vol. 3, No. 3, 1989 (Pages 739-763)
Scanning Microscopy International, Chicago (AMF O'Hare), IL 60666 USA

0891-7035/89$3.00+.00

BACKSCATTERED ELECTRON IMAGING USING SINGLE CRYSTAL SCINTILLATOR DETECTORS

R. Autrata

Institute of Scientific Instruments, Czechoslovak Academy of Sciences, 612 64 Brno, Czechoslovakia

(Received for publication March 6, 1989, and in revised form October 26, 1989)

Abstract

The image obtained by the detection of backscattered electrons (BSE) becomes an indispensable complement to the correct interpretation and more precise reconstruction of the surface of the specimen and its material composition. The BSE are carriers of information which is dependent on their angular and energy distribution. The choice of a certain type of BSE and their efficient detection make it possible to record the desired information with a different grade of quality. The knowledge of the angular and energy distribution of BSE is necessary for the adjustment of the correct position of the BSE detector with regard to the specimen and for its optimum geometrical configuration. The directional detection of a limited number of the BSE selected according to their angle and energy makes high demands on the efficiency of the detector. The paper presents BSE detectors based on single crystal aluminium oxides of YAG and YAP. Their spectral characteristics, time characteristics, detection quantum efficiency, electron resistance and mechanical, temperature and vacuum properties satisfy all demands of electron microscopy. The number of differently modified BSE detectors with single crystal scintillators allow application of various detection techniques, recording of different contrast mechanisms, combination of different detection modes (simultaneous detection), achievement of a high resolution of the BSE image.

The paper reviews some 180 published papers by other authors. Their findings and the present author's experimental results have formed the basis for backscattered electron imaging using single crystal scintillator detectors.

KEY WORDS: Scanning electron microscopy, Backscattered electrons, Single crystal scintillator detector, Angular and energy distribution, Material contrast, Topographic contrast, Channeling contrast, Resolution.

Address for correspondence:
R. Autrata
Institute of Scientific Instruments, Czech. Acad. Sci., Královopolská 147, 612 64 Brno, Czechoslovakia
Phone: 42 - 5 - 749292

Introduction

The most wide-spread mode of detection in SEM is the detection of secondary electrons (SE) by means of the scintillator photomultiplier detector according to Everhart-Thornley (1960). Though this detector detects mostly SE, a great deal of information is supplied by backscattered electrons (BSE) by their direct impact on the scintillator or as a result of their collisions with the walls of the specimen chamber and the pole piece through the mediation of SE III electrons (Everhart et al. 1959, Seiler 1968, Moll et al. 1978, Moncrieff and Barker 1978). Even when SE III is eliminated with the help of energy filters or a BSE absorption plate (Peters 1982a, 1982b) the effect of BSE cannot be fully suppressed, because there still is an SE II component due to the backscattering events in the specimen surface (Robinson 1974a). A great deal of information in the SE image is thus provided by backscattering events. There are several ways of suppressing the influence of backscattering on the SE image (Peters 1982b, 1985). The outcome is mostly detection of SE I resulting only from the interaction of primary electrons (PE) with the specimen. The resolution of the SE I image is determined by the mean escape depth of the SE (Everhart and Chung 1972) and the diameter of the incident beam. The exit position of SE I and SE II on the surface of the specimen has been visualised with the help of the emission microscope method by Hasselbach (1971,1988) and Hasselbach and Rieke (1982).

Contrary to the SE, the BSE have a source volume with a depth of about half the penetration depth of the primary beam. Nevertheless, some authors (Ong 1970a, Robinson 1974b, Crewe and Lin 1976, Moll et al. 1978, Gedcke et al. 1978) demonstrate experimental results from which high resolution of the BSE image is evident. The BSE provide information useful for the resolving power (energy low-loss BSE) (Wells 1971, 1975, Wells et al. 1973) and they are capable of producing contrast modes such as topography (Kimoto and Hashimoto 1968, Reimer and Volbert 1980a, 1980b), atomic number (Robinson 1974b, 1975), internal magnetic fields (contrast type II) (Fathers et al. 1973a, b, Yamamoto et al. 1976, Wells 1978), crystal

orientation and channeling patterns (Coates 1967, 1969, Venables and Harland 1973, Venables and Bin-Jaya 1977). For the recording of these contrast mechanisms, characteristic properties of BSE are utilized, especially their emission in all directions (Niedrig 1978a), the fact that their energy is similar to that of the incident beam (Kulenkampff and Spyra 1954) and the fact that under normal operational conditions, the emission of the BSE is higher than that of the SE for the majority of specimens. Under typical SEM operating conditions, with a beam energy 10 keV, the BSE cannot be attracted by any voltage that would not distort the incident beam. The only way to detect BSE is by the use of an efficient detector positioned in their path.

Scope of this Paper

The aim of this paper is to present a more general view of methods of BSE detection, but it is not possible to deal with every topic in detail. Many papers have been devoted to BSE detection and a review paper of this size cannot cover all aspects of the problem. The physical mechanism of backscattering was discussed in detail by Niedrig (1978a, 1978b, 1981), remarkable experimental and instrumental results were presented Robinson (1975), Newbury (1977), Reimer (1978), Wells (1979), Lange et al. (1984), Chapman and Morrison (1984), Reimer and Riepenhausen (1985). All these papers give numerous references. Excellent reviews of BSE detection were written by Wells (1977), Robinson and George (1978), Robinson (1980) and Reimer (1982). New developments in backscattered electron imaging were described by Niedrig (1988).

This paper gives a review of BSE detection systems which take advantage of individual properties of single crystal scintillators.

Why detect BSE?

The reasons for the continuously increasing interest in BSE detection are the different features of the BSE and SE images. The information provided by the BSE image is different from that of the SE image. Single crystal scintillator BSE detectors show a good signal-to-noise ratio, fast time response, high electron radiation resistance, temperature resistance, suitability for work in UHV, etc. These properties create conditions for obtaining a BSE image of a higher quality than before. The progress in the solid state semiconductor technology made it possible to enlarge the bandwidth and to improve the low energy sensitivity of semiconductor detectors. The BSE image has become an indispensable complement to the SE image of every SEM. In the following, the features of the BSE image are reviewed.

1. The BSE image can show material contrast. The highly sensitive wide angle annular BSE detector with a YAG scintillator is capable of resolving the difference of the mean atomic number 0.07 for elements with the atomic number of about 30. The highest material contrast is produced by BSE with a high energy loss, i.e., by BSE which are scattered by a perfectly polished specimen in a direction approximately opposite to that of the incident primary electron beam. The emission contrast achieved using the BSE wide angle annular detector with an angle collection of 2π sr is a mixture of material and topographic contrast. The possibilities of achieving high resolution of either type of contrast are restricted. The precondition for high resolution of the material or topographic contrast is the so-called collection contrast, i.e., contrast produced by the BSE with similar energy and angular distribution detected within a small angle of collection. Owing to the small number of electrons detected within the small angle of collection high demands are made on the detection quantum efficiency of the BSE detector. This requirement is best satisfied by the BSE detector based on single crystal scintillators.
   The material contrast can be utilized not only for material analysis, but also for the determination of the information depth of one material under the surface of another. The material contrast is of considerable importance to investigations of biological specimens marked with colloidal gold.
2. The BSE image with topographic contrast can be obtained using the detector in the low take-off angle position or using the technique of energy low-loss BSE detection with energy filtering or without it. Using energy filtering it is possible to achieve a high resolution of the image. Another technique of imaging the topographic contrast is the substraction of the BSE signals obtained from two or more detectors.
3. By means of BSE it is possible to also record other contrast mechanisms, such as type-2 magnetic contrast and channeling contrast.
4. The BSE scintillation or semiconductor detector above the specimen can be used to record an electron channeling pattern (ECP) or by the combination of vertically positioned screen the record of the simultaneous channeling contrast and EBSP is possible.
5. Edge brightness does not occur in the BSE image. A BSE detector placed above the specimen does not detect forward scattered primary electrons that produce an image with a greatly reduced edge signal. The BSE image shows more details at the edges of a specimen.
6. Compared to the SE image, the BSE image of non-conducting specimens is affected by charging to a smaller degree. The non-conducting specimen still charges, but the BSE detector does not detect this, so that the BSE image shows less charging artefacts than the SE image. As, however, Hasselbach (1988) showed, the scanning electron beam is deflected towards the positive charge. The electrostatic field around the specimen can unfavorably affect the image quality, especially from the viewpoint of resolution. Nevertheless, the BSE image of non-conducting specimens provides more details of the surface than the SE image, as e.g. Robinson (1987a) and Autrata (1984) showed.

7. The BSE image does not suffer so much from contamination effect as the SE image does. Owing to their high energy, the BSE can penetrate the contamination layer without impairing the image quality.

Physical principles of backscattering from the viewpoint of their application to the design of BSE detectors and to BSE imaging

Analyses of types, forms, and principles of electron backscattering were made by Everhart (1960), Cosslett and Thomas (1964, 1966), Archard (1961), Murata et al. (1971), Murata (1974, 1976), Niedrig (1978a, 1978b, 1981), Robinson (1975), Reimer and Tollkamp (1980), Herrmann and Reimer (1984), Reimer et al. (1986).

In order to penetrate into the problem, let us pay attention to the principles the knowledge of which is important for BSE imaging and for the design of the BSE detectors.

Types of backscattered electrons

The BSE can be considered simply from the viewpoint of their energy or from the viewpoint of their angular distribution. According to the former view, BSE are elastically scattered electrons which are characteristic of few collisions inside the specimen and of a low loss of their energy, and elastically scattered electrons which show a loss of energy which amounts to several percent in the dependence on the atomic number of the specimen. According to the latter view BSE are the so-called forward scattered electrons, which are those PE which are scattered through less than 90^0 before emerging from the specimen, and the backward scattered electrons, which are those PE which are scattered through more than 90^0 before emerging from the specimen.

Coefficient of backscattering

The coefficient of backscattering (η) is one of the most important quantities utilizable for the detection of BSE. Above all, the dependence of η on the atomic number Z of the specimen is important. It characteristically rises with increasing Z (Colby 1969). Reimer and Tollkamp (1980) determined η by measuring the BSE current using a collector. The experimentally obtained values for η reported by different authors (Reimer 1973, Cosslett and Thomas 1964, Bishop 1966, 1967) differ and do not always correspond to the evaluation by the Monte Carlo method after Kotera et al. (1981). There does not exist a complete theory for the η value so far. The evaluation of the Rutherford model of single scattering (Everhart 1960) or double scattering (Bödy 1962), or the diffusion models (Archard 1961), are only rough approximations. As reported by Heinrich (1981), the existing deviations from the monotonous course $\eta(Z)$ (which are difficult to measure owing to irregularities of the surface, even in the case of perfectly polished specimens) and the orientation anisotropy of the coefficient η (Reimer et al. 1971, Drescher et al. 1974) are obstacles for precise determination of the mean Z from the known BSE signal. The problem of the material analysis based on the measurement of the atomic number of the specimen from the $\eta(Z)$ dependence was also considered by Ball and McCartney (1981), Hall and Lloyd (1981), Marquis (1981), Robinson et al. (1984), and Robinson (1987b).

The following dependences of η can also be used with advantage for the detection of BSE.
- η increases with increasing tilt angle of the specimen and with increaseing film thickness of the specimen, if the specimen is not a bulk specimen (Kanter 1957, Drescher et al. 1970). For a certain film thickness and a certain tilt, η approaches the values of a bulk specimen.
- For bulk specimens η is approximately independent of PE energy in the range 5-100 keV (Drescher et al. 1970). Mc Affee (1976) reports that in the range of PE energies of 1 to 3 keV the differences in η values do not exceed 5%. In the range of electron energies below 5 keV, η decreases for high Z and increases for low Z with decreasing energy of PE (Reimer and Tollkamp 1980). The dependence of η on PE energy was confirmed by Monte Carlo calculations (Lödding and Reimer 1981, Reimer and Lödding (1984). For thin film specimens η increases with the increasing energy of PE (Niedrig and Sieber 1971).

Angular distribution

The knowledge of the angular distribution of BSE is important not only for the three-dimensional reconstruction of the profile of the specimen surface, but also for the determination of the detector configuration, and the size and localization of the scintillator in the specimen chamber of the microscope. Because of the straight trajectories of BSE, the contrast depends on the position of the detector. The electrons reflected in a smaller solid angle about the axis of PE provide information on material contrast, those reflected in a larger solid angle give information on the topographic contrast (Wells 1978, 1979). The BSE reflected at a large angle by a tilted specimen, the so-called low-loss electrons carrying information with high resolution, were described by Wells (1972a,b, 1974, 1975, 1980).

According to the papers published by Kanter (1957), Reimer (1979), but especially according to the excellent paper presented by Reimer et al. (1978) who rotated the detector with a small solid angle of collection (Ω) and varying take-off direction (take-off angle ξ) at a different specimen tilt angle (Reimer and Riepenhausen 1985, Reimer et al. 1986), the angular distribution of BSE normal incidence ($\varphi = 0$) can be described by Lambert's cosine law:

$$d\eta / d\Omega = \eta / \pi \cos \xi \qquad (1)$$

which results in a circle when plotting, $d\eta / d\Omega$ versus ξ in a polar diagram. There exist certain deviations for thin films of specimens with low atomic numbers, or low PE energies as shown by Monte Carlo calculations (Lödding and Reimer 1981). For bulk specimens, $d\eta / d\Omega$ depends on the atomic number. For $\varphi > 0$ the angular characteristics still show a Lambert's distribution for take-off angles $\xi < 90^0$ (Reimer et al.1984). This part of the angular distribution remains

constant in magnitude for tilt angles $\varphi < 50^{\circ}$. For larger φ this part decreases in magnitude because a large fraction of the electrons is backscattered into the maximum of the angular characteristic. If the detector lies in this direction, the material contrast disappears, but a very strong topographic contrast appears. This is the reverse of the conditions found with normal beam incidence ($\varphi = 0$) and a high take-off angle ξ when most of the detected BSE have scattering angles $\vartheta = 180^{\circ}$.

The previously published results of experimental measurements of $d\eta/d\Omega$ (Seidel 1969, Hohn 1977) and the numerically evaluated diagrams (Murata et al. 1971, Murata 1973) were made in the meridian plane. Reimer and Riepenhausen (1985) carried out measurements of angular distribution of BSE in the azimuth plane designated by the azimuth angle χ. Since the knowledge of the reflection maximum of BSE for specimens tilted at different angles φ is in both planes very important for detector localization, we made measurements of the angular distribution of BSE using a method similar to that described by Reimer et al. (1978). We replaced the scintillator by a solid-state semiconductor detector with a solid angle of collection as small as 1.10^{-2} to 1.10^{-3} sr. A stage goniometer was used to rotate the detector. The specimen was held in a stationary position. The measurement results for the azimuth plane χ_0 of positive direction are given in Fig.1, those for the meridian plane in Fig. 2. (Schematic diagram of the angles is represented in Fig. 3.) The values of the signal were corrected for the increase in η dependent on the tilt angle. It is obvious from Fig. 1 that the scattering of BSE decreases in the positive direction of the azimuth χ_{0_0} with the increasing specimen tilt. For $\varphi = 70^{\circ}$, the scattering angle ϑ is approximately 50° in the positive direction and 50° in the negative direction. If in the ideal case the angle of collection Ω is to approach the angle of scattering ϑ, then the detector bow must be adapted to the angle of scattering $\vartheta = 100^{\circ}$. This value in the azimuth plane is relatively high and implies that a scintillator of 20 mm diameter should be placed at a distance of 10 mm from the place on which PE are incident on the specimen. This distance is critically small, especially if specimens of larger sizes are used which obstruct localization of the detector. If the detector is positioned at a greater distance from the specimen, the BSE scattered within a larger solid angle are not detected by the detector. From the viewpoint of the signal the situation is not critical, because the number of the electrons scattered in a larger angle is not high. For $\varphi = 70^{\circ}$ in the meridian plane (Fig. 2), the angle of scattering ϑ is delimited by the sides of the angles $\xi_1 = 105^{\circ}$ and $\xi_2 = 150^{\circ}$, so that it is about 45°. This value is half that obtained for the azimuth plane. The shape of the cloud of BSE scattered by the tilted specimen, $\varphi = 50^{\circ}$ to 60°, resembles a cone (Fig. 3) with an elliptic

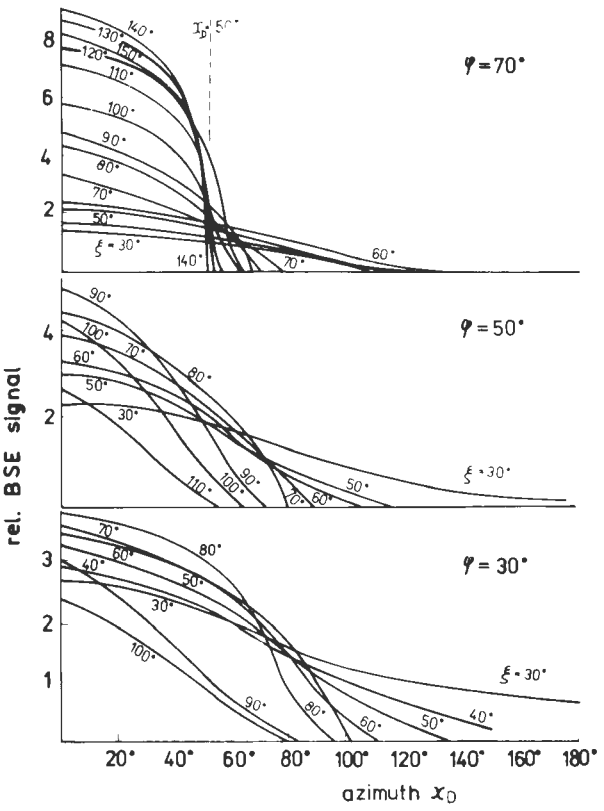

Fig. 1. BSE signal versus azimuth angle χ_0 (positive direction at specimen tilt angles $\varphi = 70^{\circ}$, 50°, 30° with the parameter of take-off angle ξ

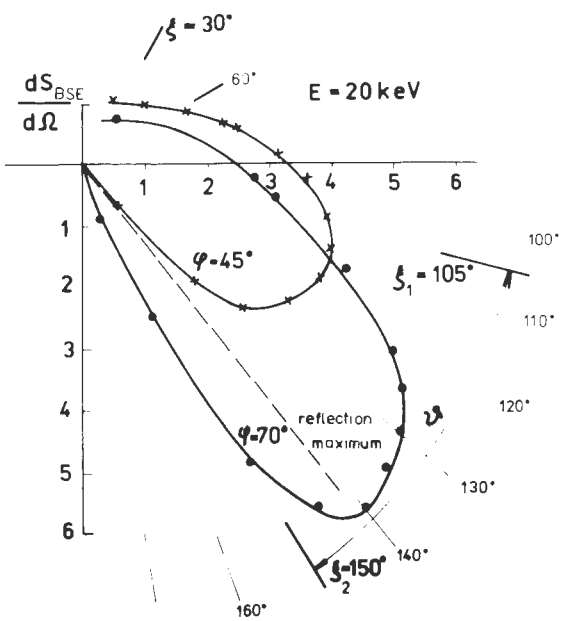

Fig. 2. BSE angular characteristic in the meridian direction at azimuth $\chi_0 = 0^{\circ}$ and specimen tilt angles $\varphi = 70^{\circ}$, 45°.

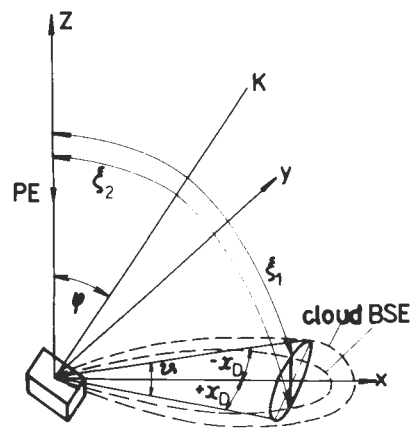

Fig. 3. Model representation of the BSE cloud emerging from the specimen tilted at $\varphi = 70^{\circ}$.

base. The base area and the height change with the changes in specimen tilt.

The knowledge of the angular distribution of BSE and of the detector position allows selection of the BSE image of certain character as will be discussed below.

Energy distribution

The knowledge of the energy distribution of BSE is necessary for the optimization of the detector configuration which allows us to obtain information dependent on the magnitude of the loss of BSE energy. The process of electron backscattering with regard to BSE energy properties were described by Kulenkampff and Spyra (1954), Everhart (1960), Archard (1961), Nachodkin et al. (1964), Thümmel (1974), Wells (1972b, 1974), Mc Affee (1976) and Niedrig (1981). The energy distribution of BSE simulated by the Monte Carlo method was described by Shimizu et al. (1972), Murata (1973), Kotera et al. (1981).

The energy distribution of electrons was mostly studied using the method of retarding the electrons after they have passed through metal foils of different thicknesses (Cosslett and Thomas 1964). A great number of relations have been derived for electron losses in the mass, but none of them gives a true picture of the actual state. For example, William's law is valid only for a narrow range of atomic numbers, and Thompson-Widdington's law shows deficiencies in nonlinear courses which differ from the Bethe (1930) courses. The process of scattering and retarding PE in the mass is very complex and the individual methods excellently surveyed by Niedrig (1981) do not allow a full description of the problem. Numerical Monte Carlo calculations (Bishop 1966, Murata et al. (1971), Murata (1973), Joy (1988) which consider the behavior of one electron with all possible collisions are more exact. They have, however, certain limitations, because they are based on laws which have some of the above shortcomings.

From this it follows that in practice the design of an efficient scintillator detector cannot be based on the theoretical models, but must be based on the experiment. In this respect it is possible to make use of the results of Wells (1971, 1975, 1979). Kulenkampff and Spyra (1954), Kulenkampff and Rüttiger (1958), Matsukawa et al. (1974) and Christou (1977). They measured by means of filtration the energy distribution of BSE for various metals and plotted diagrams which are in accordance with the experiment, but which do not agree with the theory. For example, curves calculated by the Monte Carlo method lie higher than the experimentally obtained ones, expecially for higher energies and heavier chemical elements. We concentrated in our experiments above all on the dependence of the energy distribution of BSE on the specimen tilt so that we could choose the optimum position of the detector not only according to the angular distribution of the BSE, but also according to their energy. Above all, it was necessary to verify the distribution of BSE, as far as energy is concerned, within the angle corresponding to the maximum of their reflection which is the optimum position of the detector from the viewpoint of the angular distribution.

A scheme of the measuring device is shown in Fig. 4. It consists of two scintillation BSE detectors, of which one (detector I) is equipped with a three-grid energy filter and the other (detector II) is fixed below the pole piece (to allow detection of high take-off angle electrons).

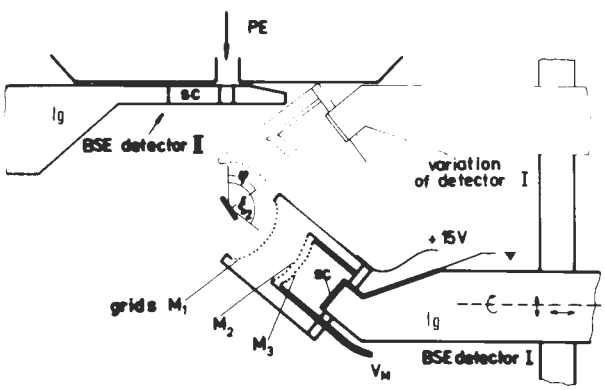

Fig. 4. Scheme of the measuring arrangement for BSE energy filtration (sc - scintillator, lg - light guide).

The position of detector I can be changed with respect to the specimen as desired. The energy resolution of the filter used amounted to 2 %. The two detectors allowed two images to be obtained simultaneously. By switching on the filter of detector I it was possible to obtain a third image as a consequence of energy filtration of BSE with an arbitrary take-off angle ξ. Fig. 5 shows curves of energy distribution (BSE rate versus BSE energy) for two take-off angles and for a specimen tilt angle $\varphi = 50^{\circ}$. Curve 2 corresponds to a take-off angle $\xi = 50^{\circ}$ (from the PE axis), curve 1 to a take off angle $\xi = 120^{\circ}$, at which, according to Fig. 2, the maximum reflection of BSE occurs. Curve 1 clearly shows that at this angle the maximum relflection of BSE is associated with the minimal energy loss.

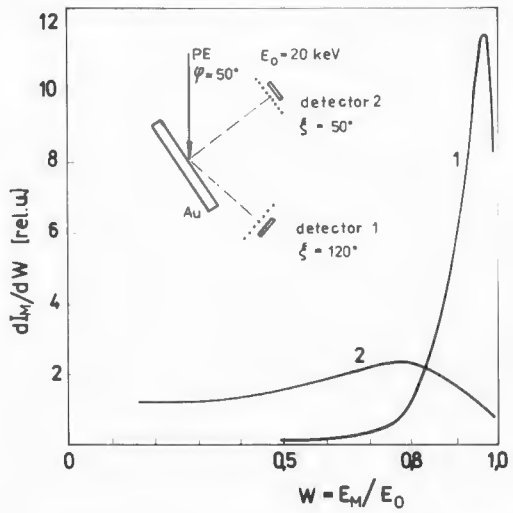

Fig. 5. BSE energy distribution at two different take-off angles.

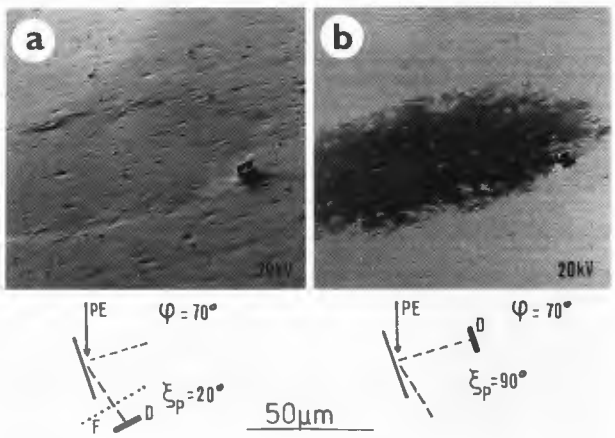

Fig. 6. Image of hole covered with thin Au, Al_2O_3, C films (D - detector, F - energy filter, φ - specimen tilt, ξ_p - take-off angle).

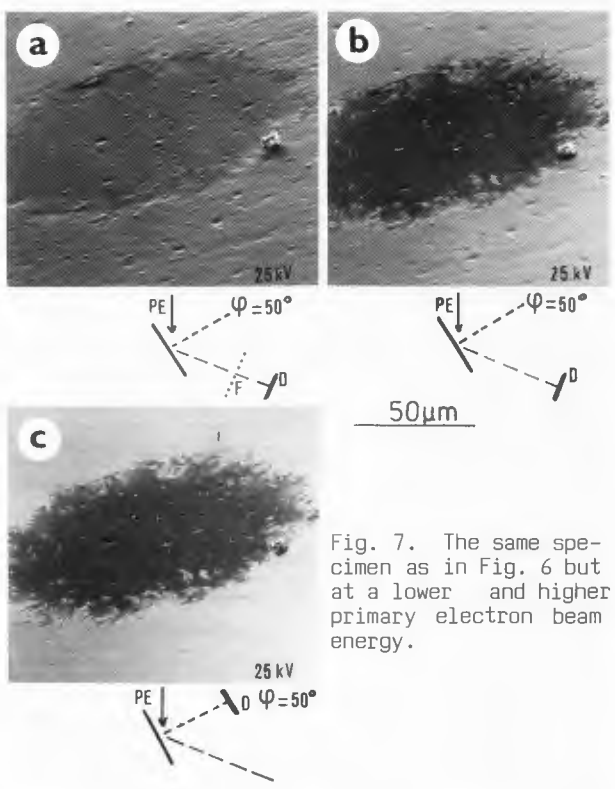

Fig. 7. The same specimen as in Fig. 6 but at a lower and higher primary electron beam energy.

Wells (1971, 1972a, 1972b) named these electrons "low take-off electrons" or energy "low-loss electrons".

The results of the energy measurements are given in Figs. 6a,b. As sample an aluminium foil was used, coated with a 30 nm thick Al_2O_3 layer and a 10 nm thick Au layer. From the reverse side a hole was etched in the aluminium foil, and from this direction the Al_2O_3 layer was coated with a 2 µm thick carbon film. Fig. 6a was obtained using an energy filter under the conditions $\varphi = 70^0$, ξ_p (from the specimen plane) = 20^0, E_M (BSE energy controlled by grid voltage M_3) = 0.96 E_0, E_0 = 20 keV, and represents the low-loss image according to Wells (1975, 1979). The good topography and the zero material contrast prove that BSE are emitted from the Au layer or the Al_2O_3 layer and represent information sources carrying high resolution. In Fig. 6b the specimen is in the same position, but the detector is in a position nearly perpendicular to the specimen surface ($\xi_p = 90^0$). In the absence of filtration voltage the detector largely detects energy high-loss BSE. The image of the hole in material contrast and the poor topography prove that the information is carried by BSE coming from the depth corresponding to the thickness of the aluminium oxide layer, the carbon layer or from even greater depth.

If the specimen tilt angle is decreased from 70^0 to 50^0, the PE can penetrate deeper into the specimen, but higher energy losses occur. An increase in PE energy from 20 keV to 25 keV has the same effect. If the percentual loss of the energy of the BSE incident upon the scintillator is maintained the same, we obtain an image as shown in Fig. 7a. Compared to Fig. 6a, the image shows already some low material contrast. If other conditions of energy filtration remain the same as for Fig. 6a, the contours of the material can be explained by the increase in the energy of PE and by the greater depth of penetration of PE into the specimen due to the lower φ. If no filtration of the energy of BSE is carried out and the specimen is in the same position, we obtain an image as shown in Fig. 7b. Curve 1 in Fig. 5 (obtained for E_0 = 20 keV, but for E_0 = 25 keV its course is not much different) indicates that the maximum rate of BSE lies in the range $E_M > 0.8\ E_0$. This means that electrons with energy losses as high as 20 % of their initial energy are detected. The BSE come from a depth greater than the thickness of the Au film (10 nm) or the thickness of the aluminium oxide film (30 nm). This manifests itself in the material contrast to which the carbon coated bottom of the hole contributes. The energy

low-loss BSE produce the topographic relief and the higher-loss BSE the material contrast in the image. If the detector is shifted to a higher take-off angle position ξ_p and if no filtration of energy is carried out, only a more marked material contrast is achieved as a result of the smaller tilt of the specimen and the higher energy of PE (compare Figs. 7c and 6b).

The aim of our experiments was to find out the difference between the low-loss images obtained with and without an energy filter, and to use a single crystal scintillator detector in this configuration. As already reported by Wells (1970) the low loss image shows a high topographic contrast if an energy filter is used. A BSE image obtained with a detector without an energy filter in the low take-off angle position shows above all topography, but under certain conditions (E_0 , φ , Ω) BSE with a certain loss of energy contribute to the material contrast (especially if a larger angle of collection Ω is used).

Resolution of the BSE image

The resolution of the BSE image is often the matter at issue. Most authors base their analyses on the theoretical model of penetration of the primary electrons into the specimen. The Monte Carlo computation (Murata 1974, Niedrig 1978a,b, 1981) shows that typically 90 % of the BSE emerge from an area of the surface whose diameter is about 0.3 of electron range. This varies with Z and beam energy E_0 . On the other hand, the experimental results of some authors (Ong 1970b, Robinson 1974b, 1975, 1980, Robinson and George 1976, 1978, Lin and Becker 1975, Takahashi 1977) show that under certain circumstances the resolution of the BSE image from a solid specimen can be considerably better than the penetration depth of PE. Most BSE images are compared with SE images formed by all components of the SE signal, i.e., including the components SE-II and SE-III which arise mainly due to BSE. If we consider that the SE-II component emerging from a depth of 1-10 nm is generated by the BSE, the output area of SE-II equals the output area of the BSE. Thus, the higher resolution can unambiguously be attributed to SE-I. Therefore, if SE-II is not subtracted from the SE signal and SE-III eliminated, the capabilities of the SE and BSE modes are not comparable from the viewpoint of resolution.

In practice, the separation of the SE components is done only rarely, but as Peters (1982a, b) showed, this technique allows one to achieve resolution corresponding to the Gaussian distribution of the spot diameter. Recently, experimental results have been presented (technical literature by Hitachi, and Cambridge Instruments) according to which the resolution in the SE mode is higher than that evaluated for the Gaussian distribution of the spot diameter of PE and the resolution in the BSE mode is higher than that evaluated for the diameter of the interaction volume of PE. No precise explanation of this discordance has been given yet. According to the traditional view of the resolution of the BSE image, the higher resolution occurs if the effective interaction volume can in some way be made smaller than the total irradiated volume in the specimen. Therefore, the resolution depends not only on the electron optical properties of the microscope and the efficiency of the detection systems, but also on the specimen itself, its preparation, tilt, etc. According to, e.g., Murata et al. (1971), Murata (1976), and Wells (1971), the information depth considerably decreases with increasing specimen tilt.

From this it follows that when a comparison of SE and BSE images is made, it is always necessary to specify the type of SE and BSE detected, because this plays an important role in the physical interpretation of the results of imaging. The comparison of the SE image formed by all components (SE-I + SE-II + SE-III) and the BSE image without specification of angular and energy properties of the BSE is of limited significance only.

Some conditions of specimen preparation which are important for the achievement of high resolution of the BSE image were specified by Mc Mullan (1953), Stewart (1962), Ong (1970b), Watanabe (1972), Abraham and De Nee (1973, 1974), Crewe and Lin (1976), Lin and Becker (1975), Becker and De Bruyn (1976) and others, and were reviewed by Wells (1977), 1979).

We concentrated our attention on the reduction of SE-III. The amount of SE-III did not exceed 10 % of the total SE signal. Compared to the SE image, the same or a higher resolution of the BSE image can be achieved under the following conditions:

1. A specimen with a very low atomic number Z is used (most biological specimens). Its surface is covered with a thin film of metal with a high Z. The BSE are emitted from only this film, because the bulk material of the specimen under this film has a very low coefficient of backscattering η . The resolution of the BSE image depends on the thickness of the thin film with high Z, on the energy of PE and on the difference of η of the materials. The image of a biological specimen in the BSE mode (using universal BSE detector in middle take-off position) and in the SE-I + SE-II mode are presented in Fig. 8.
2. On the surface of the specimen with a low Z there will be some regions with a high Z or vice

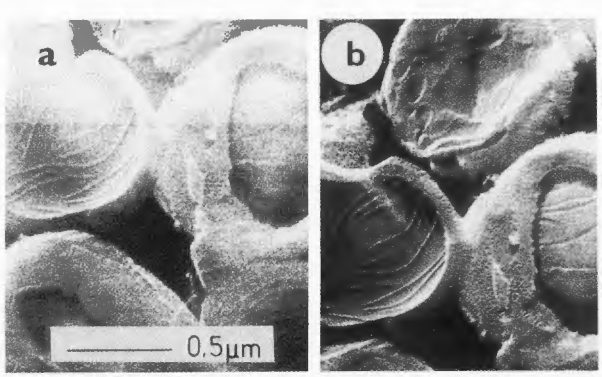

Fig. 8. Biological specimen (saccharomyces cerevisiae) in (a) SE mode, (b) BSE mode.

versa. This can be achieved by covering the specimen with a shadowing thin film of a material with a different **Z** or by producing chemical changes in the specimen or by marking the intrinsic material with particles of a metal with a different **Z** (Fig. 14). The image shows material contrast. The specimen illustrated in Fig. 9-cracks in the Au Pd layer on the carbon foil - belongs also to this group. The BSE wide angle annular detector with the collection angle of about 2/3 π sr was used.

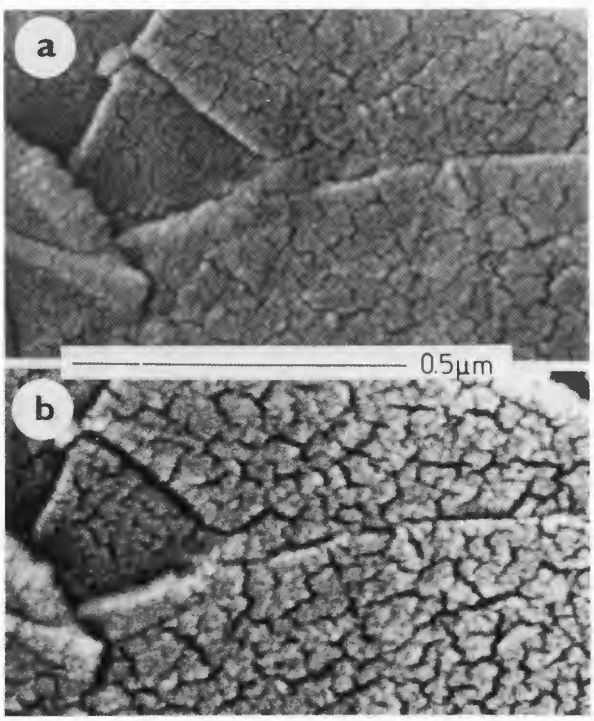

Fig. 9. Cracks in AuPd thin film on carbon foil (a) SE, (b) BSE imaging modes.

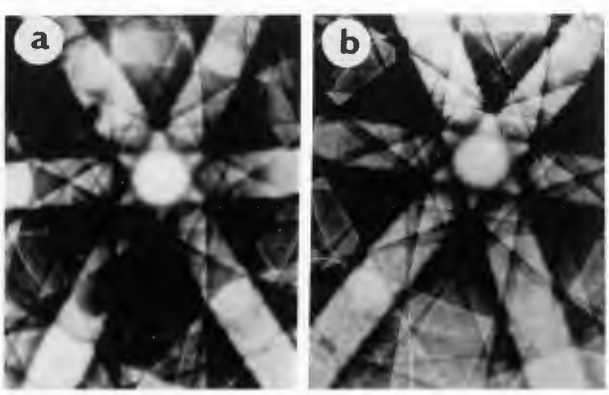

Fig. 10. ECP of silicon single crystal (111) in (a) SE mode, (b) BSE mode.

3. In the case of the single crystal specimens the BSE provide angular information with a high resolution as illustrated by ECPs in Fig. 10 in the SE-I + SE-II and BSE modes, respectively. The BSE were detected using the wide angle annular BSE detector with the collection angle of about 3/2 π sr.

4. For homogeneous specimens with average **Z**, the topographic details can be imaged with a resolution similar to that achieved by SE detection using the glancing angle of incidence of PE onto the specimen (Fig. 6). As Wells (1971, 1972a,b) Wells and Bremer (1970) showed, by detecting the energy low-loss BSE emerging from a small depth of the specimen it is possible to achieve resolution comparable with that of the SE image.

Single crystal scintillators as detectors for backscattered electrons

Detector philosophy

The BSE detector can be designed so that it detects the majority of the emitted BSE. Robinson (1974b) built a wide angle detector and designated its collection efficiency by 2π . He wrote about it: "All regions of the scintillator, which can see the specimen, contribute to the signal, although not in equal proportions" (Robinson 1987a). On the other hand, a selection of information can be made by detecting BSE in a certain direction (Wells 1970, 1974).

The philosophy of our work is based largely on the so-called directional detection, which means on the detection of the BSE emitted within certain solid angles or within a certain range of their energy.

The majority of the existing BSE detector systems aim to achieve the maximum collection efficiency which gives preconditions for a high signal-to-noise ratio. These are: annular solid state detectors according to Wolf and Everhart (1969), paired solid state detectors according to Kimoto et al. (1966), converted BSE detectors according to Moll et al. (1978), wide angle scintillator detectors according to Robinson (1974b, 1975), converted systems according to Reimer and Volbert (1980a, 1980b).

Only some authors aimed to select the BSE in a certain direction. Remarkable results were achieved with the low-loss detector using an energy filter according to Wells (1971, 1972a,b,) Wells et al. (1973). A small solid angle detector which could be positioned at any take-off angle with respect to the specimen was used by Blaschke and Schur (1974), Wells (1978) and Reimer et al. (1978, 1986).

The BSE detectors of 2π type collect at the zero tilt angle of the specimen majority of the emitted electrons, i.e., not only electrons which contribute to the material contrast, but also those with a lower loss of their initial energy which are the carriers of topographic information. These detectors have a high collection efficiency and a sufficiently high signal-to-noise ratio. They provide,however, cumulative topographic and material information.

The selection of a certain type of emitted BSE is, however, associated with a decrease in

the signal and with deterioration of the signal-to-noise ratio, because only a restricted number of BSE in the small collection solid angle is detected. The decreased signal-to-noise ratio can be balanced by increasing the sensitivity and transfer efficiency of the detector. Therefore, we set out to build detectors with maximum light output efficiency and geometrical variability capable to provide a sufficient signal when the BSE in the small collection solid angle are detected. In other words, we decided to prefer directional information of the BSE to cumulative information.

At present, there are two types of efficient detection systems - the solid state semiconductor and the scintillator photomultiplier. We preferred the latter, because it had lower noise, larger bandwith, sensitivity to low energies and made it possible to apply high voltage to its interaction surface.

The most important part of a well operating scintillator photomultiplier detector is an efficient scintillator. Plastic scintillators have a short lifetime and show rapid degradation of material after the impact of signal electrons (Pawley 1974), powder scintillators cannot be shaped, have low mechanical strength and limited lifetime. Therefore we concentrated our attention on the choice and implementation of an efficient scintillator (Autrata et. al. 1984).

Scintillators

The scintillator photomultiplier detector consists of a scintillator, a light guide and a photomultiplier. All three parts must satisfy certain requirements, regardless of whether they form the Everhart-Thornley (1960) SE detector or a BSE detector. From the analysis of the scintillator photomultiplier detector made by Schauer and Autrata (1979) and from the behavior of individual components of the detector chain described by Baumann and Reimer (1981) and Comins and Thirlwall (1981) it has become obvious that the value of detection quantum efficiency (DQE coefficient) of the detector depends above all on the electron-photon energy transfer which takes place in the scintillator. Since this transfer must be rapid (if television frequencies are to be used), only the plastic scintillator or the P 47 powder phosphor (yttrium silicate activated with cerium) can be used. But both materials show certain deficiencies when used for the BSE detectors.

Autrata et al. (1978) prepared single crystal scintillators based on yttrium aluminium garnet activated by trivalent cerium ($YAG:Ce^{3+}$) and yttrium aluminium perovskite activated by trivalent cerium ($YAP:Ce^{3+}$), respectively (Autrata et al. 1983a). Both types of single crystal scintillators meet all requirements of electron microscopy. Moreover, they can be shaped by cutting, grinding and polishing, and this is especially advantageous for the construction of BSE detectors. Their properties were described in detail elsewhere (Autrata et al. 1983b, 1983c).

Properties of YAG and YAP scintillators

Efficiency of electron - photon energy transfer

The absolute value of quantum efficiency of $YAG:Ce^{3+}$ and $YAP:Ce^{3+}$ single crystals has not been measured yet. Takeda et al. (1980) give 7 % quantum efficiency for polycrystalline YAP (powdered), Bril et al. (1971) report 4 % for polycrystalline YAG (powdered phosphor P 46) and Pawley (1974) 6 - 8 % for powdered phosphor P 47.

Relative efficiency

The values quantum efficiency are not generally applicable, because the technologies of phosphor powders (but also of single crystal scintillators) are so different that phosphor of individual producers or even of the production batches of one producer can differ considerably. It is sufficient to make a relative comparison of the efficiencies of scintillators prepared from these materials. The efficiency of P 47 phosphor ($2\ mg/cm^2$, E_0 = 10 keV, I_0 = 500 pA by Riedel de Haën) proved comparable with the efficiency of the single crystal YAG or YAP plate of 0.7 mm thickness whose base facing the light guide is ground and the base hit by the incident electrons is provided with a reflecting aluminium layer (made by Monokrystaly Turnov, Czechoslovakia). The relative efficiency of the scintillator depends not only on the technology of its preparation, but also on the conditions under which the light emerges. These conditions can be influenced by reflecting, antireflecting and diffusion layers or by crystals of different shapes from which light is comming in different direction and with different intensity. For example, the light output signal from the bottom base of the single crystal YAG disc is less than one half of the light output signal of a conical scintillator with an apical angle of 130^{o} (Autrata and Mejzlík 1988a). From this it follows that it is not possible to compare efficiencies of the P 47 phosphor, plastic scintillator and YAG and YAP single crystals in general. It is always necessary to give the particular type of scintillator, its shape, the direction in which the light is measured, optical adaptations of the scintillator, etc.

Detective quantum efficiency

The detective quantum efficiency of the scintillator photomultiplier detector (primary beam is incident directly on the scintillator) is expressed by the ratio $DQE = (S/N)^2_{output} / (S/N)^2_{input}$ (square of signal-to-noise ratio at detector ouput to square of signal-to-noise ratio at detector input). On the basis of the method suggested by Pawley (1974), an excellent analysis of this problem was made by Comins et al. (1978), Comins and Thirlwall (1981), Baumann and Reimer (1981), Thirlwall and Comins (1981) and Browne and Ward (1982) using the P 47 or the plastic scintillator. The DQE of the detector with the single crystal YAG scintillator in the form of a disc was measured by Autrata et al. (1983b) and Oatley (1985). The DQE values of about 0.8 (Autrata) and of about 0.7 (Oatley) at the primary beam energy of 10 keV are higher than that of the P 47 scintillator. Nevertheless, it is not possible to compare absolute values of DQE, because they contain various errors in PMT characteristics and other measuring components. The comparing of the DQE values loses its importance. A better method of specifying the merit of the scintillator photomultiplier system is the measurement of the mean number of electrons per pulse reaching the first

dynode of the photomultiplier.

And now to the problem that still remains open. As already mentioned in the preceding section and in an earlier paper (Autrata and Mejzlík 1988a), the light output signal strength of the single crystal scintillator disc is lower in the direction of the bottom base than in the direction of the peripheral area. By making appropriate optical adaptations or by shaping the scintillator, e.g., to form a cone, it is possible to considerably increase the light output signal in the direction of the bottom base. This proves that with the YAG disc currently used high optical losses occur and the light is propagated also in other directions than in the desired one. The amount of light collected in a certain (let us say "required") direction does not correspond to the amount of light generated in a quantized manner. This is understandable from the viewpoint of laws of geometrical optics (index of refraction of YAG 1.84), when light is propagated within the solid angle of 4π . It is most probable that owing to optical adaptations of the scintillator (reflection, antireflection, shaping) which result in an increase in the light signal in the desired direction, the DQE coefficient or the mean number of electrons per pulse reaching the first dynode of PMT increases. But if the output pulses are large, they are of no avail if many pulses have been lost.

Time charasteristics

By time characteristics we mean the rise time and the decay time of the cathodoluminescent process. It is the decay time which is critical when using a scintillator in a SEM. If television frequencies higher than 10 MHz are to be used this decay must be shorter than 100 ns. According to the graphic-numerical method by Stevenson (1977), a multicomponent equation (Autrata et al. 1983b) was derived which considers both the decay time (interval between the end of excitation and the decrease in the intensity of cathodoluminescence to a value which is **e** times lower; **e** is the base of the natural logarithm) and other time constans representing the long-term components of the afterglow. The decay time of YAG is 80 ns, of YAP 40 ns, which suits television frequencies and there is still a large reserve. A comparison of the afterglow and sensitivity characteristics of the YAG single crystal and P 46 powder scintillators at 100 kV and 1 MeV primary beam energy was made by Koichi et al. (1988).

Spectral properties

The single crystal YAG or YAP scintillator performs two important functions simultaneously. It is an efficient source of the light signal in an appropriate wavelength region and a light guide which does not absorb light just in the wavelength region of its own emission. The absorbtion spectrum (Kvapil et al. 1980) of YAG shows a broad absorption band with its maximum at 460 nm and a narrow band at 340 nm. The absorption spectrum YAP has only one absorption band lying at energies close below the absorption edge (260-330 nm). The emission spectrum of YAG shows a characteristic peak at 560 nm wavelength with 145 nm band half-width. The characteristic emission band of YAP lies at the boundary of the ultraviolet and the visible spectrum region with a maximum at a wavelength of 378 nm and a half-width of 50 nm (Autrata et al. 1983c). For the design of the BSE detectors it is very important to know the value of the so-called self-absorption which actually means absorption of its own emission. The self-absorption in a 5 mm thick single crystal amounts to 9 % for YAG and to 20 % for YAP.

Lifetime and damage resistance

The YAG and YAP single crystals show resistance to electron beam damage. Their properties change neither due to long-term incidence of high energy electrons (1 MeV) nor due to a high current density of the electron beam (1.10^{-5} Acm^{-2}). Under the extreme conditions, the maximum changes in efficiency range from to 3 % after several thousand hours of performance. If irradiated by an extremely high current of electrons ($\sim$1 A), the single crystal warms up and above 400^{0} C its luminescent efficiency decreases owing to thermionic extinction. The change is, however, reversible. After the single crystal has been cooled down, it works with its original efficiency. If the surface of the single crystal is in any way contaminated, it can be cleaned chemically, or in the case of more severe contamination by polishing and activated by dipping it into phosphoric acid (for 2 min. at 100^{0} C). At room temperature the YAG and YAP single crystals show resistance to all acids, bases and solvents (Schauer et al. 1985). Since the are very hard, they are cut with diamond charged saws and their surface is treated with diamond paste.

Different types of BSE detectors with a single crystal scintillator

The single crystals scintillators of YAG and YAP considered to be a new generation of scintillators for EM (Seiler 1983, Pawley 1984, Comins and Thirlwall 1981, Niedrig 1988) can be shaped and this allows the design of detectors for a wide range of applications. The possibility of shaping single crystal scintillators with respect to the optimum angle of collection of BSE and with respect to the optimum propagation of light towards the PMT is utilized both for BSE and for SE detectors. Pawley (1984) used in LVSEM SE detectors with two scintillators of hemispherical shape, Autrata and Mejzlík (1988a, 1989) showed that the YAG single crystal scintillator of conical shape gives the maximum light output signal and modified the Everhart-Thornley SE detector. As BSE detection is not yet usual in every SEM, let us pay attention, above all, to the BSE detectors. Some scintillators for this type of detectors are presented in Fig. 11.

Wide angle annular detector

The wide angle annular detector is the type of detector for which the solid angle of collection can be altered by altering the working distance. The basic part of this detector consisting of the scintillator and the light guide is shown in Fig. 12. The scintillator can be a disc with a hole to enable the passage of PE. The scintillator diameter and the working distance

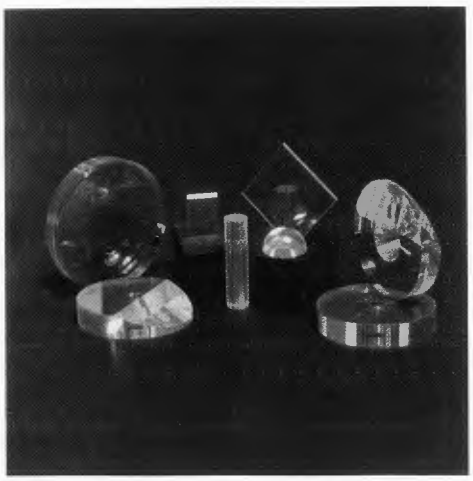

Fig. 11. Single crystal scintillators for BSE detectors.

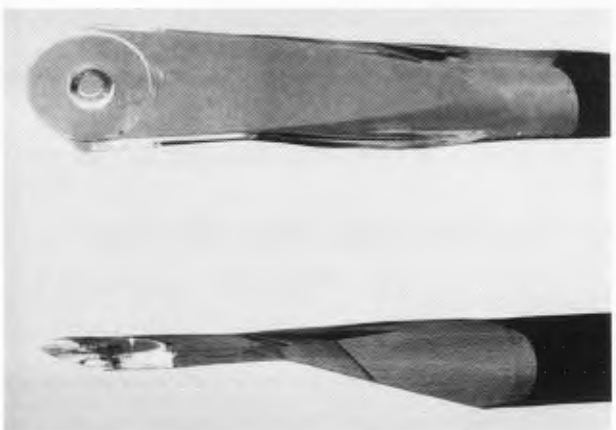

Fig. 12. Wide angle annular detector.

are important for the adjustment of the optimum solid angle of collection of BSE. This type of detector is intended for imaging the material contrast. It should collect BSE scattered by an untilted specimen in an angle demarcated by the sides of the take-off angle ξ not greater than $\pm$ 35° measured from the axis of PE. From the viewpoint of the position of the detector this type of detection is called the high take-off angle detection. If the solid angle collection of BSE is decreased, the BSE emitted from the specimen at lower scattering angles which lose a smaller amount of their energy are cut off, so that mostly energy high-loss BSE which are the carriers of the material contrast are detected. By decreasing the collection efficiency given by the smaller solid angle of collection the topographic information is suppressed. At the same time the number of detected BSE decreases, which results in a decreased signal-to-noise ratio. The optimal solution of the problem is achieved with a single crystal scintillator. The diameter of the hole in the scintillator to enable the passage of PE and through which BSE escape without being detected by the scintillator is important. The minimum diameter is determined by the requirements of minimum magnification. For this reason the hole is to be situated as close to the objective aperture as possible. In order to fulfill this requirement as well as possible it is advantageous to shape the hole as a cone broadening towards the specimen. The advantage of the conical hole is that it prevents the astigmatism of the primary electron beam, and, compared to this, the loss of the BSE detected due to the higher coefficient of backscattering η on the tilted plane of the scintillator is negligible. Astigmatism mostly occurs when the hole is too high (the path of PE too long) and its surface not perfectly conductive or when the center of the hole is not in the axis of PE. Unfavourable optical properties of the conical hole are negligible (Autrata et al. 1986).

The conical hole or a larger hemispherical cavity ground in the scintillator allow the specimen to be located close to the detector and therefore detection of BSE over an angle of collection of 2π sr, so that the majority of the BSE emitted from the specimen are detected (Robinson 1974b). The signal-to-noise ratio is maximized but the resultant image contains integrated information on both material and topographic contrast. The sensitivity to the material contrast is decreased.

Another advantage of the wide angle annular detector is that it is possible to make the light signal from the peripheral area of the YAG disc scintillator propagate in the direction of the light guide and the PMT. As described in an earlier paper (Autrata and Mejzlík 1988a), light generated in the scintillator propagates in all directions. Only a minor part passes through the scintillator - light guide boundary in the desired direction. The major part is reflected by the walls or is absorbed. The light output signal towards the PMT can be substantially increased if the walls of the scintillator and the scintillator - light guide boundary are appropriately adapted. For example, if the scintillator in the wide angle annular detector is made conductive by replacing the usually used aluminium layer deposited on both bases by an indium tin oxide layer of a thickness which does not absorb the energy of the BSE, the light output signal is increased by 80 %. If the peripheral area of the disc covered with the antireflecting layer is polished and the peripheral area diverted from the light guide is matted, the light output signal is increased by another 15 %. And if, finally, a diffusion reflecting layer (e.g., MgO) is deposited on the diverted peripheral area and on the scintillator - light guide boundary the light output signal is increased to three times the light output signal achieved with the unadapted detector.

Of no less importance is the shape and the surface finish of the light guide. Bauer and Egg (1984) used a light guide in the form of a strip

to which the YAG disc was cemented. They were interested in material contrast deep inside the specimen and though they achieved remarkable results, the detector with the strip light guide with rectangular profile shows losses three times those obtained with a light guide with circular profile. The reason is the number of reflections which is by some orders of magnitude higher, and the absorption of light along the edges of the strip light guide.

The image of material contrast obtained with the optically adapted wide angle annular detector with an angle of collection $2/3\,\pi$ sr is shown in Fig. 13a. In the left-hand part of the image copper with the atomic number 29.00 is shown, in the right-hand part of the image the copper-zinc phase with a mean atomic number 29.07 can be seen. Fig. 13b is an SE image.

As Walther et al. (1984) showed, the wide angle annular detector can be used with advantage for quantitative evaluation of particles marked with colloidal gold. Fig. 14 shows images of protein particles on a blood cell in the SE and BSE mode, respectively. If the specimen is prepared under specific conditions, it is possible to resolve 1000 protein A gold particles per μm^2. On this example it is possible to demonstrate the correctness of one of the conditions defined by Wells (1977) for the achievement of the BSE image with a high resolution: "If a sample consists of small high-Z regions in a low-Z matrix, then the BSE can show these inclusions with a good resolution".

Position detector

Knowing the angular and energy distribution of BSE one can place the BSE detector into various positions with respect to the specimen and to select accordingly the information. The signal profile changes with the altering tilt of the specimen and the position of the detector. The influence of the specimen tilt can be best simulated using a sphere the signal profiles of which were demonstrated by Reimer and Pfefferkorn (1977), Lin and Becker (1975), George and Robinson (1975), and Robinson and George (1976). These papers did not pay attention to the detector position which determines the height of the signal from a certain point of the sphere and in the case of SE detection they did not mention the individual types of the SE detected. Later Reimer et al. (1984, 1986) concerned themselves with these aspects. A model of a signal profile is illustrated in Fig. 15. It shows three positions of the BSE detector. The PE are incident on the sphere in points A, B, C and the BSE emitted from these points give different information corresponding to their angular and energy distribution. The detector in the high take-off angle position gives information about the material contrast, the detector in the middle take-off position provides mixed information on the material and surface topography and the detector in the low take-off angle position supplies information on the topographic contrast (Ikuta 1983).

The interpretation of the BSE signal in the papers by Robinson (1974b, 1975) is based on a detector of the 2π type which detects at a large solid angle of collection, $2\,\pi$ sr. Here, the majority of the BSE produce the material contrast and part of electrons with a lower loss of energy carry topographic information (dependent on the working distance). This necessitates perfectly polished surfaces of the specimen when material contrast is imaged. However, the detector can be positioned at a greater working distance where it detects less electrons with a lower loss of energy. The detector designed by Moll et al. (1978, 1979) and modified by Reimer and Volbert (1979, 1980b), which makes use of the conversion of BSE into SE, detects BSE in a higher take-off angle position. The detector provided with a second converter plate (Reimer 1979, Reimer and Volbert 1980a) allows separation of the topographic and material contrast. The specimen is tilted in this case. The second converter plate can be placed in any position with respect to the specimen. The advantage of this arrangement is that no additional PMT and video path are needed. The BSE detection depends on the number of SE produced by the conversion and on the efficiency of the SE detector.

The position detectors with single crystal YAG scintillators are shown in Fig. 16. Each of the detectors is capable of detecting BSE in the high and low take-off angle positions (Fig. 16b), or in the high and middle take-off angle positions (Fig. 16a). The choice of signal is made with a mechanical diaphragm mounted on a flange of the detector in front of the PMT as described by Autrata (1984) for the combination of the SE and BSE detectors. The area of the scintillators is small, because it is desirable to collect a narrow beam of BSE carrying the desired kind of information corresponding to their angular and and energy distribution. The low collection efficiency is no obstacle to the achievement of sufficient signal, because the sensitivity of detectors with single crystal scintillators is sufficiently high.

Performance of the BSE detector in the high take-off angle position was discussed and illustrated in Fig. 13a. The BSE image obtained with the detector in the low take-off angle position ($\xi_p = 10 - 30^o$, $\varphi = 70^o$) is presented in Fig. 17b. The higher topographic contrast compared to the SE image (Fig. 13b) is due to the high tilt angle of the specimen and due to the type of low-loss energy BSE detected with the detector in the low take-off angle position. The image in Fig. 17a was obtained using the detector in the middle take-off angle position ($\xi_p = 40 - 60^o$, $\varphi = 50^o$). This image shows both material and topographic contrast. The material contrast is reduced and the topographic contrast is increased in comparison with the image in Fig. 13a. It is possible to interpret the BSE image more correctly, if the specimen tilt angle φ and the sides of the take-off angle ξ_p are given.

Paired detector

The paired detector consisting of two complete detection units allows substraction of the BSE signal of one detection unit from the BSE signal of the other detection unit. Addition of signals of both detection units is also possible. The difference signal provides the topographic contrast, the sum signal the material contrast.

The method proposed by Kimoto et al. (1966) required two solid state semiconductor detectors.

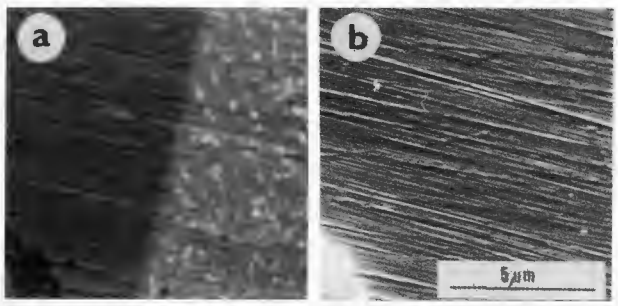

Fig. 13. Material contrast for atomic number resolution capability of the $2/3\,\pi$ sr wide angle annular detector of the copper-zinc phases.

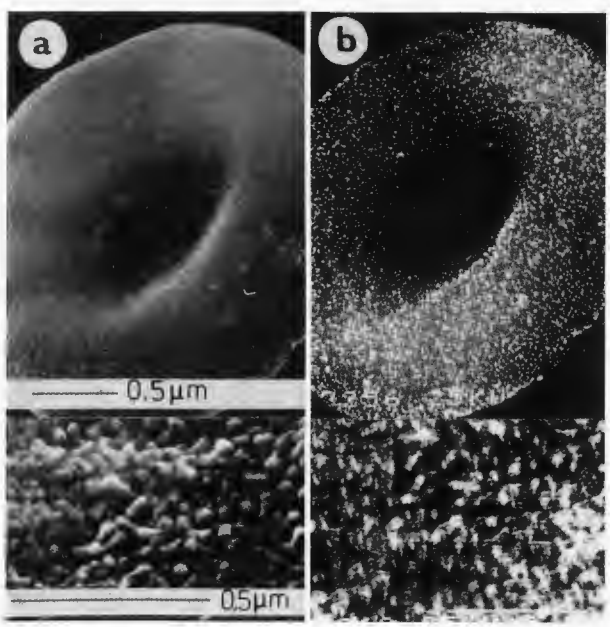

Fig. 14. Image of protein A gold 15 nm marked surface antigens on red blood cell by (a) SE detector and (b) wide angle annular BSE detector (With courtesy of P. Walther, Max-Planck-Inst., Dortmund).

Lebiedzik and White (1975) used four semiconductor detectors and Jackman (1980) and Lange et al. (1984) four scintillation detectors. A two detector system for SE or BSE/SE conversion consisting of two ETDs was described by Reimer and Volbert (1980a).

Two types of paired detectors with single crystal scintillators are presented in Figs.18a,b. Fig. 15a shows two scintillation discs, Fig. 15b two semi-discs which can be pressed to each other. The touching area is provided with a dielectric reflecting layer which reflects light into that detection unit in which it was generated.

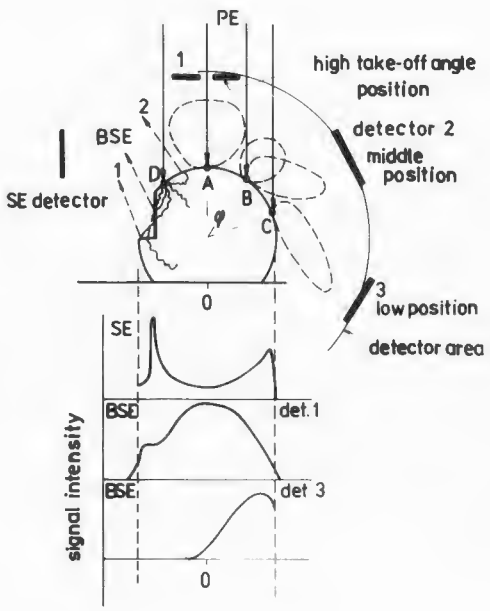

Fig. 15. Profiles of SE and BSE signals in the dependence on the specimen tilt.

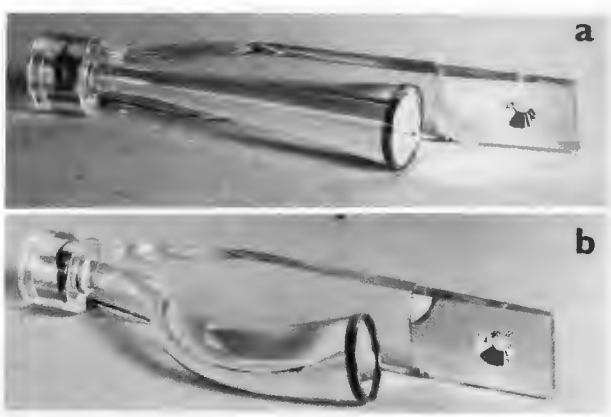

Fig. 16. Position detectors. (a) combination of high and middle take-off angles, (b) combination of high and low take-off angles.

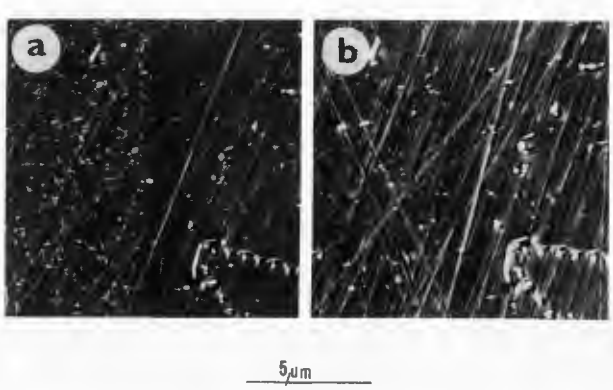

Fig. 17. BSE images obtained with detector in (a) middle take-off angle position, (b) low take-off angle position.

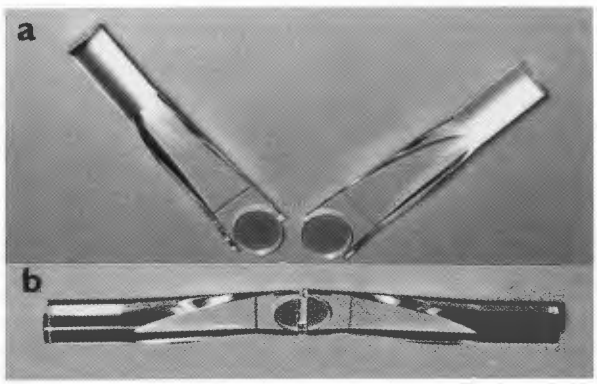

Fig. 18. Paired detectors.

The sum signal of the semi-disc paired detector is equal to that of the wide angle annular detector (identical geometry).

Detectors for STEM

The detector system of the scanning transmission electron microscope (STEM) has some specificities: different electron optical system, specimen chamber geometry, specimen character and specimen position. The STEM is equipped with detectors which also detect transmitted electrons in two image modes of the dark or bright field. Detectors with single crystal scintillators are suitable for the detection of these electrons in both image modes.

Most BSE detectors used in the STEM are, in principle, solid state semiconductor discs (Reimer et al. 1979) or channel-multiplier discs (English et al. 1973). To a smaller extent a scintillator detector is used. An interesting solution was suggested by Wiggins (1978) and Wiggins et al. (1979) who used a single crystal scintillator (CaF_2) and replaced the light guide in the annular detector by a mirror reflecting the generated light onto PMT. Since the specimen is placed in the gap of the objective lens, there is not much space left for the detector. Koike et al. (1971) positioned their BSE detector (specimen tilted) behind the lens. Autrata et al. (1986) positioned the detector in the lens above the specimen.

As obvious from Figs. 19a, b, also the BSE detectors in STEM can be based on the principle of the wide angle annular detector (Fig. 19a), or the position detector (Fig. 19b). The diameter of the annular scintillator can be as large as 8 mm for the solid angle of collection of the BSE of $4/3\,\pi$ sr. As the working distance of the specimen cannot be altered, the angle of collection of BSE can be decreased using a metal shielding foil attached to the scintillator or using a scintillator of a smaller diameter. The hole in the scintillator to enable PE to pass through should be of conical shape (to prevent astigmatism) and it must be perfectly conducting. Its minimum diameter is given by the compromise between the requirements for minimum magnification and the collection efficiency of the BSE. The optical adaptation of the

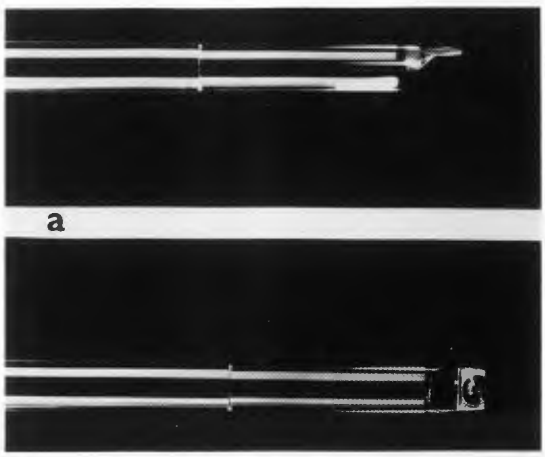

Fig. 19a. BSE detectors for STEM. Frontal and side views of the wide angle annular detector.

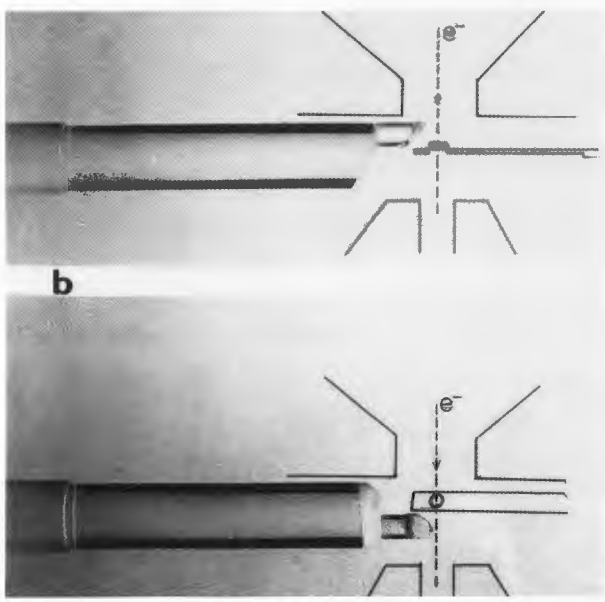

Fig. 19b. Position detector for high to middle take-off angles and for high to low take-off angles.

detector by means of the reflecting, antireflecting and diffusion layers results in a more than two-fold increase in the signal-to-noise ratio. The resolution of the BSE image depends on the character of the thin film specimen and on the operational capability of the microscope. This can be best documented by comparison of images obtained under equal conditions using different imaging modes (Fig. 20). For a given specimen, the resolution does not differ from the resolution in the SE and BF imaging modes. The resolution of 3 nm in the BSE mode for a biological specimen is illustrated in another paper (Autrata et al. 1986).

The wide angle annular detector can easily be replaced by the position detector (Fig. 19b).

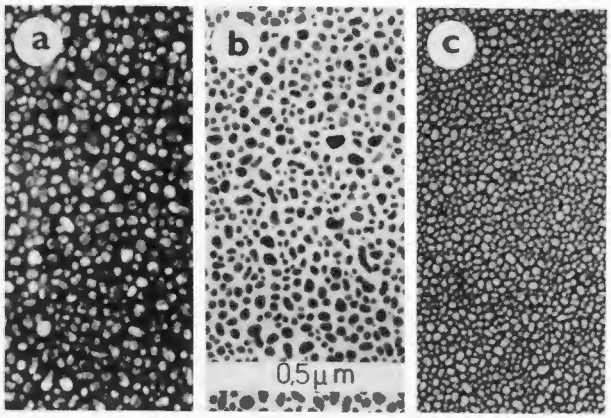

Fig. 20. Gold islands on carbon thin film in (a) SE, (b) BF, (c) BSE imaging modes.

By rotating about the light guide axis the elliptical scintillator plate can change its position with regard to the specimen. Using a specimen in a tilted position and the detector in the low take-off angle position one can detect BSE which provide an image with features similar to those resulting from the angular and energy distribution of BSE. It is however necessary to pay attention to the fact that the mechanisms of backscattering for thin films and bulk materials are different. As described by Hohn et al. (1976), Schmoranzer et al. (1975) and Niedrig (1978b, 1981), the angular distribution of BSE gets more flat with decreasing film thickness, so that the maximum reflection corresponding to a certain scattering angle decreases. Conditions for energy distribution also change. There is not much experience with the position detector in STEM so far. The image in Fig. 21a shows only the material contrast obtained using the detector in the high take-off angle position, the image in Fig. 21b shows the topographic contrast obtained using the detector in the low take-off angle position.

Ring detector

An interesting approach to the detection of BSE in the defined zenith and azimuth angles was described by Hejna (1987, 1988). A ring scintillator with a light guide surrounds the specimen in the azimuth angle of 360°. By changing the working distance of an untilted specimen it is possible to change the zenith angle of detection and to detect topographic changes in the chosen angle of collection Ω delimited by the sides of the take-off angle ξ_{sp} within 0 - 60°. It is also possible to use a shielding metal foil to delimit the azimuth angle of detection (Hejna 1988). Taking advantage of knowledge of reconstruction of surface topography by means of a two detector system (Lebiedzik 1979, Lebiedzik et al. 1979, Volbert and Reimer 1980, Reimer and Tollkamp 1982, Suganuma 1985) or a four detector system (Jackman 1980, Lange et al. 1984, Carlsen 1985, Reimer and Riepenhausen 1985), Hejna and Reimer (1987) used a ring detector divided into two or four segments to make a more precise reconstruction of the surface topography along a linescan.

The advantages of the ring detector become evident when the BSE detection for an untilted specimen is carried out. The azimuth angle of 360° ensures a high BSE collection efficiency in the azimuth plane while in the zenith plane the topographic information is chosen. The ring detector shows higher collection efficiency and better directivity than similar detector systems described earlier (Wells 1970, 1974, Schur et al. 1974, Harris et al. 1976, Zeldes and Tassa 1979) which used the ET detector positioned at different zenith angles of detection.

The detector with a single crystal YAP ring scintillator (Hejna 1988) has a very good signal-to-noise ratio. Autrata and Hejna (1989) modified the detector so that it permits simultaneous SE and BSE detection in the low voltage SEM. The principle of the modified detector (Fig. 22) intended for low voltage operation is that a high voltage of 10 kV is supplied to the internal peripheral area of the ring scintillator and a suction grid is introduced to which a low positive or a low negative voltage is supplied. The suction of the signal electrons in the azimuth angle of 360° and the symmetric electrostatic field have such an effect that the primary electrons are not deflected irregularly from the axis and the low energy SE or BSE sucked by the high field to the

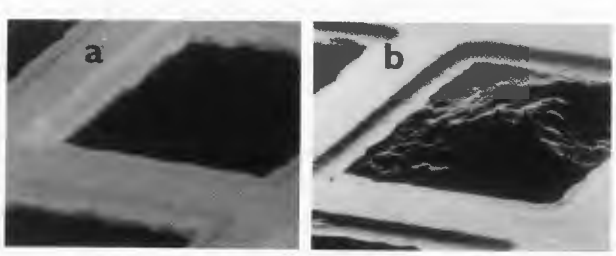

Fig. 21. Carbon replica of a biological specimen on the gold grid detected by the position BSE detector in STEM. (a) high take-off angle position, (b) low take-off angle position.

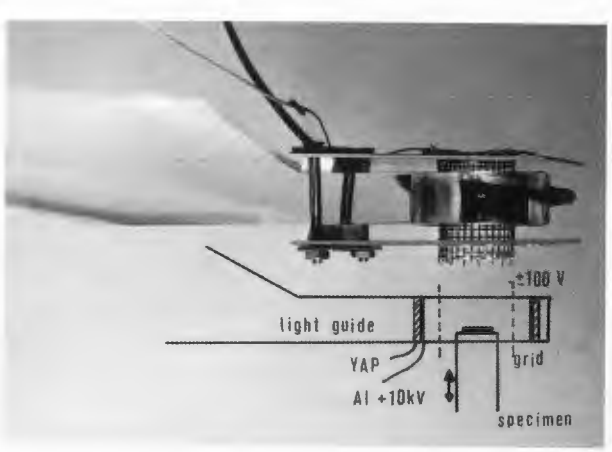

Fig. 22. Experimental design of ring detector for simultaneous SE and BSE detection in LVSEM.

scintillator do not intersect the axis of the PE beam. The results of the SE and BSE detection at 0.8 keV energy of PE are shown in Figs. 23a,b, respectively. The detector is capable of operating at any low voltage, provided the properties of the electron optical system influencing the PE beam in the column of the microscope allow this. It is obvious from Fig. 20 that with the modified ring detector with an accelerating voltage of 10 kV applied to its scintillator, in the low take-off angle position, $\xi_p = 0^o - 20^o$, better topography is obtained with BSE than with SE.

Though the experiments with the modified ring detector are in the stage or a preliminary study of its advantages and disadvantages, it seems that this detector can help us resolve the problem of detection in the LVSEM as discussed by Pawley (1984, 1988), Pawley and Scala (1986) and Postek et al. (1988). The advantages of this type of detector are symmetric field, good signal-to-noise ratio, possibility of detecting BSE with low energy PE and separating the SE and BSE signals.

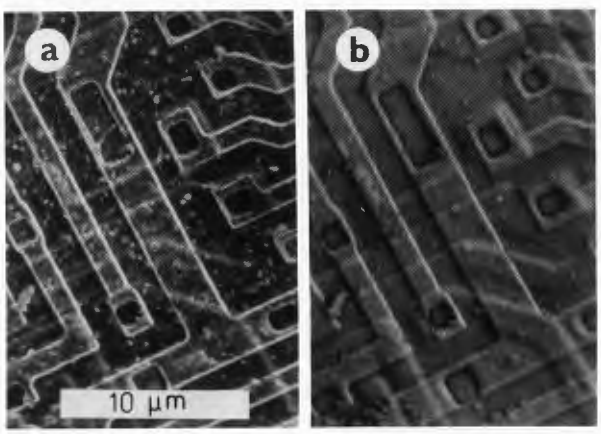

Fig. 23. Image of integrated circuit obtained with a modified ring detector in (a) SE mode, (b) BSE mode at primary electron beam energy 0.8 keV. Not covered with a conductive layer.

Universal detector

The above mentioned detectors are equipped with fixed light guides which do not allow a sufficiently variable adjustment of the position of the scintillator. To design a detector with a fixed light guide, it is necessary to know the geometrical dimensions of the specimen chamber of the microscope into which it is to be built. In the detector shown in Fig. 24 the fixed light guide has been replaced by a flexible fibre optics light guide provided with connectors on both sides. One is connected to the PMT, the other is intended for attachment of different types of light guide pieces with a scintillator. The input connector is fixed in a holder outside the specimen chamber of the microscope. It allows changes in position of the scintillator with regard to the specimen.

The whole light guide part is made of quartz

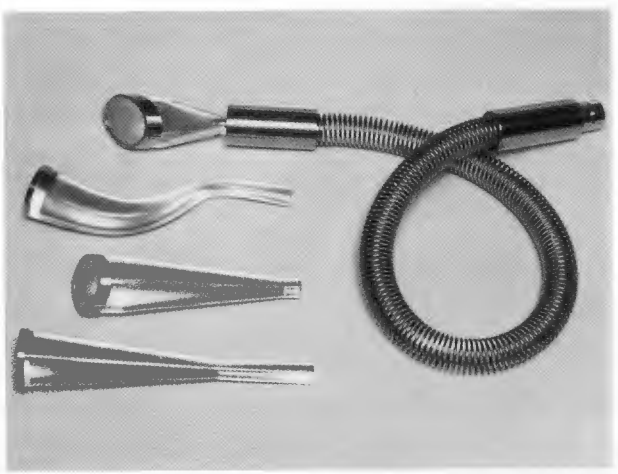

Fig. 24. Universal detector with interchangeable light guide pieces.

glass. The scintillator is covered with a very resistant conducting ITO layer, and is connected to the light guide using a holder. No cement is used. These adaptations make it possible to use the detector not only in UHV microscopes, but also for the "in situ" method, when for example thermally treated specimens are investigated. The detector is resistant to temperatures up to 1500°C. The decrease in luminescent efficiency begins to show itself from 400°C upwards (thermal quenching of luminescence). The process is reversible. The luminescent efficiency returns to its original value after the scintillator has been cooled down. The detector can be used with advantage for the recording of channeling contrast during simultaneous thermal treatment of crystalline specimens. A good quality of channeling contrast by means of BSE is achieved even without ion cleaning of the specimen surface, because as follows from Fig. 25 the BSE image does not suffer so much from contamination effects as the SE image does.

Channeling contrast is based on angular dependent variations of the BSE yield with angle, which are caused by diffraction of BSE at the lattice planes of the crystalline specimens. This effect has been extensively studied by Hashimoto et al. (1962), Boersch et al. (1964), Booker et al. (1967), Hirsch and Humphreys (1970), Reimer et al. (1971), Newbury (1974) and others and has been comprehensively reviewed by Niedrig (1978a). The detection of channeling contrast with a small adjustable BSE detector was introduced by Reimer et al. (1978).

The alteration of the position of the universal BSE detector using the flexible light guide enables alteration of relative contrast of specimens with different crystalline orientation. The maximum channeling contrast can be observed at the take-off angle $\xi_p = 90^o$.

Using the arrangement shown in Fig. 26 it is possible to detect simultaneously channeling contrast and electron backscattering channeling patterns (EBSP) by the universal detector.

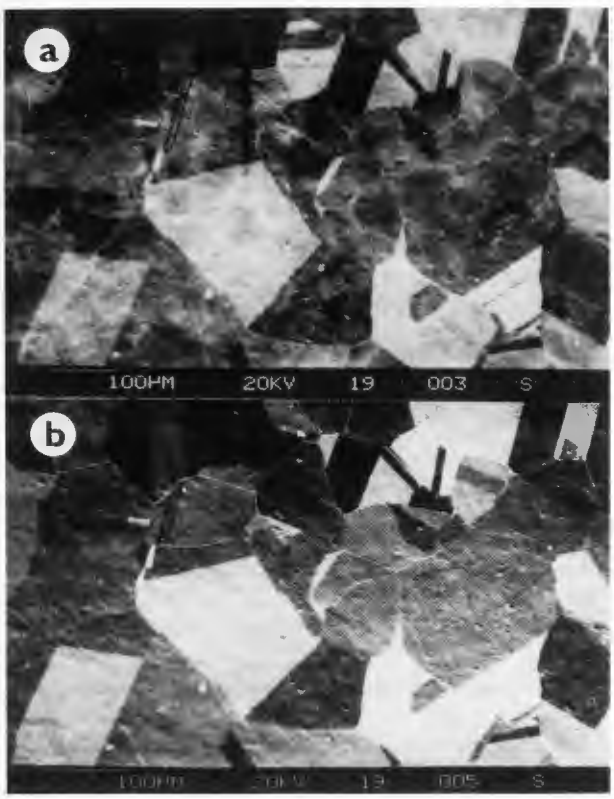

Fig. 25. Channeling contrast of polycrystalline copper ("in situ" temperature treatment) in (a) SE mode, (b) BSE mode.

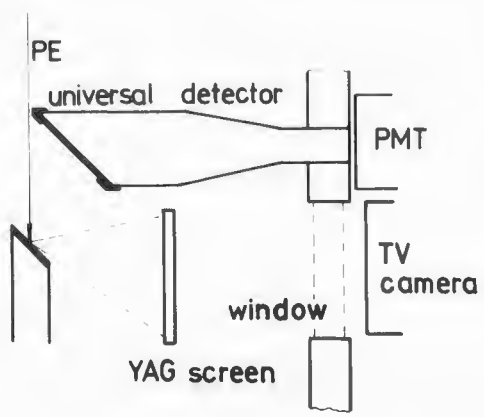

Fig. 26. Detector assembly for simultaneous imaging of channeling contrast and EBSP.

This technique was developed by Venables and Harland (1973), Venables et al. (1974, 1975), Venables and Bin-Jaya (1977), Harland et al. (1978). A stationary electron beam is focused upon a tilted specimen (φ = 50 - 80°). Some of the incident electrons are slightly inelastically scattered within the specimen and subsequently elastically backscattered toward the single crystal YAG screen. These backscattered electrons (Bragg reflected) produce a pattern on the screen which is characteristic of both the orientation and the structure of the specimen. The YAG screen has a high resolution which can be observed using a photographic or a TV camera, or it can be amplified using an image amplifier. Owing to the high temperature and radiation resistance of the YAG screen as well as the detector, this technique is suitable for work in the UHV SEM and for the "in situ" method.

Fig. 27 illustrates channeling contrast of copper with crystalline grains of 20 - 100 µm size after the process of thermal recrystallization without ion cleaning. The figure shows also an EBSP obtained of the single crystal YAG screen (Ø = 35 mm, d = 1 mm) which corresponds to two areas of the copper specimen with different crystallographic orientation. The image was recorded from the screen using a TV camera and photographed from the monitor screen. The image was formed intentionally under operating conditions of the microscope (E_0 = 10 keV, I_0 = 5.10^{-10} A, φ = 60°) that were not optimal for the given detection mode. The aim was to document that the detector assembly is capable of achieving an acceptable quality of image even at a low energy and a low current of the primary electron beam.

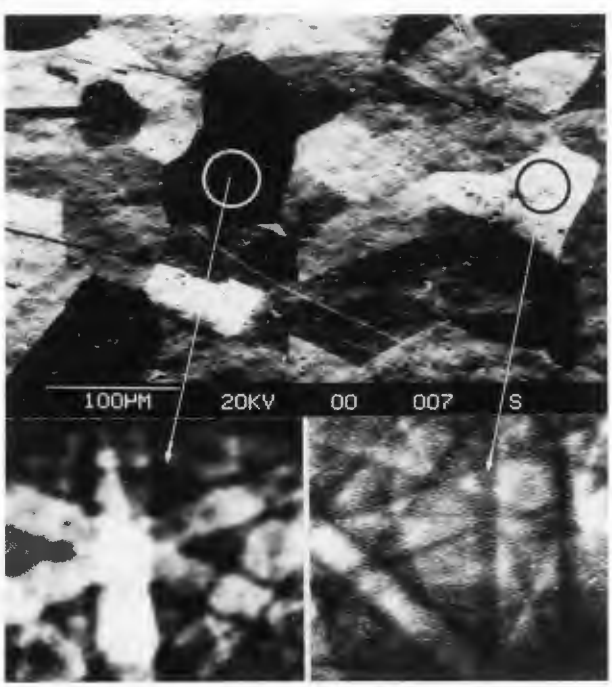

Fig. 27. EBSPs corresponding to the crystallographic orientation of selected crystal grains of copper specimen.

Double detectors

This designation stands for detector compact assemblies which in addition to BSE detection are capable of giving information also in another mode. The assembly can be connected to one PMT

and the choice of signal is made with the diaphragm positioned in front of the PMT. This group of detectors does not include multiple detector systems which detect either SE or BSE at various angles, with different energy, and which sum or substract signals as suggested by Kimoto et al. (1966), Lebiedzik and White (1975), Jackman (1980), Reimer and Volbert (1982), Lange et al. (1984), Reimer et al. (1984) and others. The double detector assembly should be simple, cheap and easily applicable to any SEM.

A typical detector assembly was designed by Wells and Bremer (1970). The collector turret rotating about one PMT permitted detection in four modes. Autrata (1984) designed a double detector, consisting of a BSE detector in the high take-off angle position and a miniaturized Everhart-Thornley detector, which enables simultaneous detection of BSE and SE. As obvious from Fig. 28. separate light guides in one flange are connected to one PMT signal in front of which a choice of signal is made with a diaphragm. The detector is of advantage to users of microscopes which have only one video channel.

Another detector assembly which also makes use of the choice of signal in front of the PMT permits simultaneous detection of BSE and cathodoluminescence (CL) (Boyde, private communication) (Fig. 29). The wide angle elliptical BSE scintillator made from the YAG single crystal houses in one focus the specimen and in the other focus the window of the fibre optics light guide. The light guide of the BSE scintillator and the fibre optics lead to the PMT in front of which the choice of the BSE or the CL signal is made. The elliptically shaped scintillator ensures a large angle of collection of BSE. The scintillator is coated with a reflecting aluminium layer which reflects the light emitted by the specimen toward the light guide window from where it is guided to the PMT. For the mirror system designed, e.g., by Bond et al. (1974), and Hörl (1975) no scintillation material is used. The advantage of this assembly is the possibility of simultaneous detection of BSE and CL without any adaptation of the detector construction. For example, semiconductor detectors require a special version of detector with a high purity quartz optical window to record the CL image.

The single crystal YAG disc can be used in another double detector as the transmission attachment for the bright and dark field imaging mode in SEM. So far several devices have been built to adapt the conventional SEM to the transmission mode. Most of them were based on the detection of converted secondary electrons (Crawford and Liley 1970). Another way of detection was based on the use of a scintillator detector below the specimen and the contrast aperture (Wolf et al. 1972) or without the aperture (Swift and Brown 1970).

The principle of the above-mentioned attachment is illustrated in Fig. 30. The detector comprises a PIN diode which is cemented on a single crystal scintillation disc of YAG. The light is guided by the fibre optics light guide towards the PMT. The whole device is fixed to the goniometer stage so that it can be moved simultaneously with the stage. The PIN diode collects the unscattered or inelastically scattered electrons of the primary beam (bright field). The elastically scattered primary electron beam (dark field) is detected by the scintillator round the diode. The action of the detector was described and the obtained images were presented by Autrata and Mejzlík (1988b).

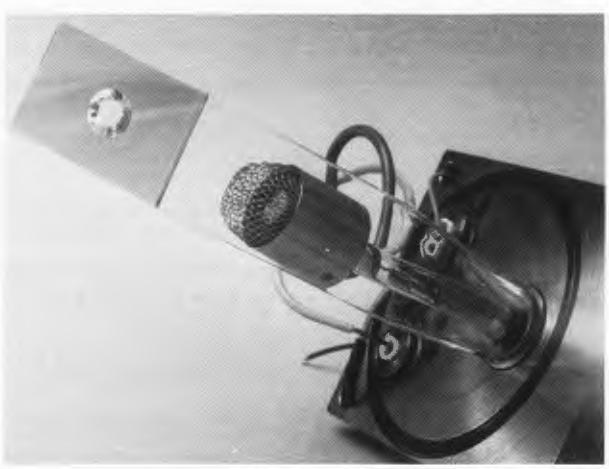

Fig. 28. Double detector of BSE and SE.

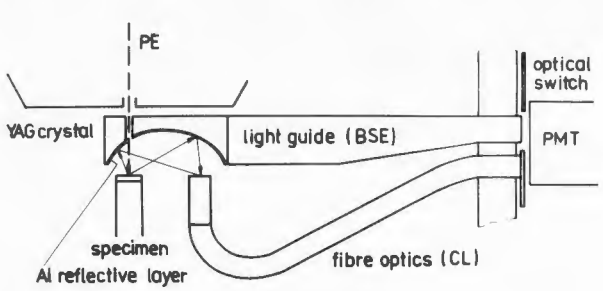

Fig. 29. Double detector of BSE and CL.

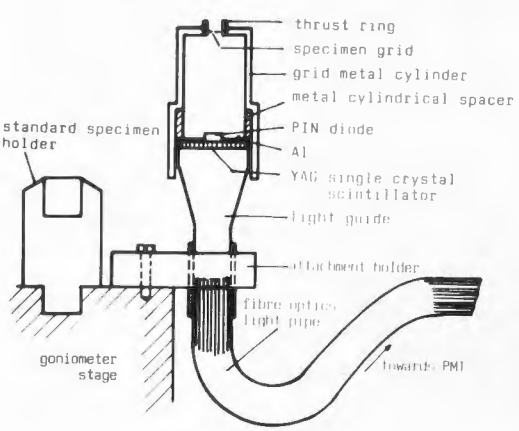

Fig. 30. Transmission attachment for bright and dark field imaging mode in SEM.

References

Abraham JL, De Nee PB (1973) Scanning Electron microscope histochemistry using backscattered electrons and metal stains. Lancet - 1:1125-1127.

Abraham JL, De Nee PB (1974) Biochemical applications of backscattered electron imaging - One year's experience with SEM histochemistry. Scanning Electron Microsc. 1974:251-258.

Archard GD (1961) Backscattering of electrons. J. Appl. Phys. 32:1505-1509.

Autrata R (1984) A double detector system for BSE and SE imaging. Scanning 6:174-182.

*Autrata R, Hejna J (1989) Ring detector for simultaneous SE and BSE detection in LVSEM. To be published in Scanning.

Autrata R, Mejzlík J (1988a) Problems of light output from single crystal scintillators. 9th Eur. Congr. EM York 1988 Proc. Vol 1 128-129.

Autrata R, Mejzlík J (1988b) Transmission attachment for bright and dark field imaging mode in SEM. 9th Eur. Congr. EM York 1988 Proc. Vol 1 121-122.

*Autrata R, Mejzlík J (1989) A modification of E-T secondary electrons detector with a single crystal scintillator. Scanning, in press.

Autrata R, Schauer P, Kvapil Jos, Kvapil Ji (1978) A single crystal of YAG:Ce - new fast scintillator in SEM. J. Phys. E: Sci. Instrum. 11: 707-708.

Autrata R, Schauer P, Kvapil Ji, Kvapil Jos (1983a) A single crystal of $YAlO_3:Ce^{3+}$ as a fast scintillator in SEM. Scanning 5:91-96.

Autrata R, Schauer P, Kvapil Jos, Kvapil Ji (1983b) Single crystal aluminates - a new generation of scintillators for scanning electron microscopes and transparent screens in electron optical devices. Scanning Electron Microsc. 1983; II:489-500.

Autrata R, Schauer P, Kvapil Jos, Kvapil Ji (1983c) Cathodoluminescent efficiency of $Y_3Al_5O_{12}$ and $YAlO_3$ single crystals in dependence on Ce and other dopants concentration. Crystal Res. and Technol. 18:907-913.

Autrata R, Schauer P, Kvapil Ji, Kvapil Jos (1984) Single crystal electron detectors. 8th Eur. Congr. EM Budapest 1984 Proc Vol 1 617-625.

Autrata R, Walther P, Kriz S, Müller M (1986) A BSE scintillation detector in the (S)TEM. Scanning 8:3-8.

Ball MD, Mc Cartney DG (1981) The measurement of atomic number and composition in an SEM using backscattered detectors. J. Microscopy 124:57-68.

Bauer B, Egg B (1984) An optimized Backscattered Electron Detector for the Scanning Electron Microscope. Prakt. Met. 21:460-471.

Baumann W, Reimer L (1981) Comparison of the noise of different electron detection systems using a scintillator-photomultiplier combination. Scanning 4:141-151.

Becker RP, De Bruyn PPH (1976) Backscattered electron imaging of exogenous peroxidase activity in rat bone marrow. Scanning Electron Microsc. 1976; II:171-178.

Bethe HA (1930) Zur Theorie des Durchgangs schneller Elektronen durch Materie. Ann. Physik (Leipzig) 5:325-400.

Bishop HE (1966) Some electron back-scattering measurements for solid targets. Proc. Fourth Int. Congr. X-ray Opt. Mic. Orsay 1965 (Hermann-Press Paris) p 153-158.

Bishop HE (1967) Electron scattering in thick targets. Brit. J. Appl. Phys. 18:703-715.

Blaschke R, Schur K (1974) Der Informationsgehalt des Rückstreubildes im Raster-Elektronenmikroskop. BEDO 7:33-52.

Boersch H, Jeschke G, Raith H (1964) Dynamische Theorie der elastischen Elektronenbeugung unter Verwendung komplexer Atomfaktoren. Z. Phys. 181: 436-452.

Bödy ZT (1962) On the backscattering of electrons from solids. Brit. J. appl. Phys. 13:483-485.

Bond EF, Beresdorf D, Haggins HH (1974) Improved cathodoluminescence microscopy. J. Microscopy 100:271-282.

Booker GR, Shaw AMB, Whelan MJ, Hirsch PB (1967) Some comments on the interpretation of the "Kikuchi-like reflection patterns" observed by scanning electron microscopy. Phil. Mag. 16:1185-1191.

Bril A, Blasse G, Gomes de Mesquita AH, Porter JA (1971) Fast Phosphors for colour television. Philips Techn. Rev. 32:125-130.

Browne MT, Ward JFL (1982) Detectors for STEM and the measurement of their quantum efficiency. Ultramicroscopy 7:249-262.

Carlsen IC (1985) Reconstruction of true surface-topographies in SEM using backscattered electrons. Scanning 7:169-177.

Chapman JN, Morrison GR (1984) Detector systems for transmission electron microscopy. J. Microsc. Spectrosc. Electron 9:329-340.

Christou A (1977) Correlation of low loss electron images with Auger images of semiconductor substrate surfaces. Scanning Electron Microsc. (1977); I:159-166.

Coates DG (1967) Kikuchi-like reflection patterns obtained with the scanning electron microscope. Phil. Mag. 16:1179-1184.

Coates DG (1969) Pseudo Kikuchi orientation analysis in the SEM. Scanning Electron Microsc. 1969:27-40.

Colby JW (1969) Backscattered and secondary emission as ancillary techniques in electron probe and analysis. Adv. Electronics Electron Phys. 6: 117-196.

Comins NR, Thirlwall JT (1981) Quantitative studies and theoretical analysis of the performance of the scintillation electron-detector. J. Microscopy 124:119-133.

Comins NR, Hengstberger MME, Thirlwall JT (1978) Preparation and evaluation of P-47 scintillators for scanning electron microscope. J. Phys. E. Sci. Instrum 11:1041-1047.

Cosslett VE, Thomas RN (1964) Multiple scattering of 5-30 keV electrons in evaporated metal films. Br. J. Appl. Phys. I - 15:883-907; II - 15:1283-1300; III (1965) - 16:779-796.

Cosslett VE, Thomas RN (1966) Penetration and energy loss of electrons in solid targets. In: The Electron Microprobe ed. Wiley. New York, 1966, 248 -268.

Crawford BJ, Liley CRW (1970) A simple transmission stage using the standard collection system in the scanning electron microscope. Jour. Phys. E Sci. Instrum. 3:461-462.

Crewe AV, Lin PSD (1976) The use of backscattered electrons for imaging purposes in a scanning electron microscope. Ultramicroscopy 1:231-238.

Drescher H, Reimer L, Seidel H (1970) Rückstreukoeffizient und Sekundärelektronenausbeute

*See pp 763.

10-100 keV Elektronen und Beziehungen zur Raster-Elektronenmikroskopie. Z. angew. Phys. 29:331-336.

Drescher H, Krefting ER, Reimer L, Seidel H (1974) The orientation dependence of the electron backscattering coefficient of gold single crystal films. Z. Naturforsch. 29a:833-837.

English CA, Griffith BW, Venables JA (1973) The applications of channel plates in transmission and scanning electron microscopes. Acta electronica 16:43-57.

Everhart TE (1960) Simple theory concerning the reflection of electrons from solids. J. Appl. Phys. 31:1483-1490.

Everhart TE, Chung MS (1972) Idealised spatial emission distribution of secondary electrons. J. Appl. Phys. 43:3708-3711.

Everhart TE, Thornley RFM (1960) Wide - band detector for microampere low-energy electron currents. J. Sci. Instrum. 37:246-248.

Everhart TE, Wells OC, Oatley CW (1959) Factors affecting contrast and resolution in a scanning electron microscope. J. Electron Control 7: 97-111.

Fathers OJ, Jakubovics JP, Joy DC (1973a) Magnetic domain contrast from cubic materials in the scanning electron microscope. Phil. Mag. 27:765-768.

Fathers DJ, Jakubovics JP, Joy DC, Newbury OE, Yakowitz H (1973b) A new method of observing magnetic domains by scanning electron microscopy. Phys. Stat. Sol. (a) 20:535-544.

Gedcke DA, Ayers JB, De Nee PB (1978) A solid state backscattered electron detector capable of operating at TV scan rates. Scanning Electron Microsc. 1978; I:581-594.

George EP, Robinson VNE (1975) Topographic intensity profiles in the scanning electron microscope-cubes. J. Microscopy 105:289-279.

Hall MG, Lloyd GE (1981) The SEM examination of geological samples with a semiconductor backscattered electron detector. Amer. Mineralogist 66:362-368.

Harland CJ, Klein JH, Akhter P, Venables JA (1978) Electron backscattering patterns in a field emission gun scanning electron microscope. Electron Microscopy 1978 (Toronto) Vol I 564-565.

Harris LB, Moncrief DA, Robinson VNE (1976) High resolution examination of uncoated insulators by SEM applied to grain boundaries in sodium chloride. Phys. Stat. Sol. (a)35:371-377.

Hashimoto H, Howie A, Whelan MJ (1962) Anomalous electron absorption effects in metal foils. Proc. Roy. Soc. A 269-280.

Hasselbach F (1971) Untersuchung der Verbreiterung von fokussierten Elektronenstrahlen durch Streuung in dünnen und dicken Objekten mit dem Elektronenemissionsmikroskop. 15. Tagung für Elektronenmikroskopie 1971 in Karlsruhe. Abstract published in Mikroskopie 28 (1972) 352.

Hasselbach F (1988) The emission microscope: A valuable tool for investigating the fundamentals of the scanning electron microscope. Scanning Microscopy 2:41-56.

Hasselbach F, Rieke U (1982) Spatial distributions of secondaries released by backscattered electrons in silicon and gold for 20-70 keV primary energy. 10th Int. Cong. EM Hamburg, Proc. Vol 1, 253-254.

Heinrich KFJ (1981) In: Electron Beam X-Ray Microanalysis. Van Nostrand-Reinhold, New York. p 105.

Hejna I (1987) A ring scintillation detector for detection of backscattered electrons in the scanning electron microscope. Scanning Microscopy 1(3)983-987.

Hejna I (1988) Optimization of the ring scintillation detector for backscattered electrons in the scanning electron microscope. EUREM 88 York Proc. Vol I, Ch I 119-120.

Hejna I, Reimer L (1987) Backscattered Electron Multidetector Systems for Improved Quantitative Topographic Contrast. Scanning 9:162-172.

Herrmann R, Reimer L (1984) Backscattering coefficient of multi-component specimens. Scanning 6:20-29.

Hirsch PB, Humphreys CJ (1970) The dynamical theory of scanning electron microscope channeling patterns. Scanning Microsc. 1970:449-455.

Hohn FJ (1977) Angular dependence of electron intensities backscattered by carbon films. Optik 47:491-494.

Hohn FJ, Kindt M, Niedrig B, Stuth B (1976) Electron backscattering by thin top layers on bulk materials. VIth Eur. Congr. EM Jerusalem 1976 Proc. Vol I 383-385.

Hörl EM (1975) Verbessertes Ellipsenspiegel-Detektorsystem für die Kathodolumineszenz-Rasterelektronen-Mikroskopie. BEOO 8 Remy Münster 369-374.

Ikuta T (1983) Disappearance of topographical contrast in the backscattered electron image in scanning electron microscopy. Appl. Phys. Lett. 42:533-534.

Jackman J (1980) New scanning electron microscope depends on multifunction detector. Ind. Res. and Dev. ISSN-01160-4074 Philips Eindhoven.

Joy DC (1988) An introduction to Monte Carlo simulations. 9th Eur. Congr. EM York 1988. Proc Vol 1 23-32.

Kanter H (1957) Zur Rückstreuung von Elektronen im Energiebereich von 10-100 keV. Ann. Phys. 20:144-166.

Kimoto S, Hashimoto H, Suganuma T (1966) Stereoscopic observation in scanning microscopy using multiple detectors. In: The Electron Microprobe Mc Kinley TO, Heinrich KFJ, Wittry OB (eds) Proc. Symp. Washington, O.C. John Wiley and Sons New York 480-489.

Kimoto S, Hashimoto H (1968) On the contrast and resolution of the scanning electron microscope. Scanning Electron Microsc. 1968: 63-78.

Koichi I, Hibino M, Maruse S, Autrata R (1988) Afterglow and sensitivity characteristics of YAG single crystal and P46 powder scintillators. Annual meeting of Japan. Soc. EM, paper no. 3-II-20, page 150 (in Japanese).

Kotera M, Murata K, Nagami K (1981) Monte Carlo simulation of 1-10 keV electron scattering in a gold target. J. Appl. Phys. 52:997-1003.

Kvapil Jos, Kvapil Ji, Blažek K, Zikmund J, Autrata R, Schauer P (1980) The luminescence efficiency of YAG:Ce phosphors. Czech. J. Phys. B 30:185-192.

Koike H, Neno K, Suzuku M (1971) Scanning device combined with conventional electron microscope. Proc. EMSA 28-29. Claytors Publ. Div, Baton

Rouge LA.

Kulenkampff H, Spyra W (1954) Energieverteilung rückdiffundierter Elektronen. Zeitschrift für Phys. 137:416-425.

Kulenkampff H, Rüttiger K (1958) Untersuchung der Energieverteilung rückdiffundierter Elektronen an dünnen Metallschichten. Zeitschrift für Phys. 152:249-260.

Lange M, Reimer L, Tollkamp C (1984) Testing of detector strategies in scanning electron microscopy by isodensities. J. Microscopy 134:1-12.

Lebiedzik J (1979) An automatic topographical surface reconstruction in the SEM. Scanning 2:230-237.

Lebiedzik J, White EW (1975) Multiple detector method for quantitative determination of microtopography in the SEM. Scanning Electron Microsc. 1975:181-188.

Lebiedzik J, Edwards R, Philips R (1979) Use of microtopography capability in the SEM for analysing fracture surfaces. Scanning Electron Microsc. 1979; II:61-66.

Lin PSD, Becker RP (1975) Detection of backscattered electrons with high resolution. Scanning Electron Microsc. 1975:61-70.

Löding B, Reimer L (1981) Monte Carlo Rechnungen im Energiebereich 1-20 keV. BEDO 1981, 14: 315-324.

Marqius PM (1981) The crystallisation of calcium aluminate glasses. J. Microscopy 124:257-264.

Matsukawa T, Shimizu R, Hashimoto H (1974) Measurement of the energy distribution of backscattered kilovolt electrons with a spherical retarding-field energy analyser. J. Phys. D. 7:695-702.

McAffee WS (1976) Determination of energy spectra of backscattered electrons by use of Everhart's theory. J. App. Phys. 47:1179-1184.

McMullan D (1953) An improved scanning electron microscope for opaque specimens. Proc. IEE 100 Pt. II 245-259.

Moll SH, Healey F, Sullivan B, Johnson W (1978) A high efficiency, nondirectional backscattered electron detection mode for the SEM. Scanning Electron Microsc. 1978; I:303-310.

Moll SH, Healey F, Sullivan B, Johnson W (1979) Further development of the converted backscattered electron detector. Scanning Electron Microsc. 1979; II:149-154.

Moncrieff DA, Barker PR (1978) Secondary electron emission in a scanning electron microscope. Scanning 1:195-197.

Murata K (1973) Monte Carlo calculations on electron scattering and secondary electron production in the SEM. Scanning Electron Microsc. 1973; 267-276.

Murata K (1974) Spatial distribution of backscattered electron in the scanning electron microscope and electron microprobe. J. Appl. Phys. 45: 4110-4117.

Murata K (1976) Depth resolution of the low - and high - deflection backscattered electron images in the scanning electron microscope. Phys. Stat. Sol. (a)36:527-532.

Murata K, Matsukawa T, Shimizu R (1971) Monte Carlo calculations on electron scattering in a solid target. Jap. J. Appl. Phys. 10:678-686.

Nachodkin NG, Ostrouchov AA, Romanovskij VS (1964) Effect of the atomic screening factor on the inelastic scattering of electrons. Soviet Physics - Solid State 7:1014-1016.

Newbury DE (1974) The origin detection and uses of electron channelling contrast. Scanning Electron Microsc. 1974:1037-1057.

Newbury DE (1977) Fundamentals of scanning electron microscopy for physicist: contrast mechanism. Scanning Electron Microsc. 1977; I:553-568.

Niedrig H (1978a) Physical background of electron backscattering. Scanning 1:17-34.

Niedrig H (1978b) Backscattered electrons as a tool for film thickness determination. Scanning Electron Microsc. 1978; I:841-858.

Niedrig H (1981) Simple theoretical models for electron backscattering from solid films. Scanning Electron Microsc. 1981; I:29-45.

Niedrig H (1988) recent developments in backscattered electron imaging. Proc. EUREM 88 York Vol I Ch 4 225-230.

Niedrig H, Sieber P (1971) Rückstreuung mittelschneller Elektronen an dünnen Schichten. Z. angew. Phys. 31:27-31.

Oatley CW (1985) The detective quantum efficiency of the scintillator/photomultiplier in the scanning electron microscope. J. Microscopy 139: 153-166.

Ong PS (1970a) Contrast and resolution in scanning electron microscopy using backscattered electrons. Proc. EMSA 1970 Claitors Baton Rouge, LA. 392-393.

Ong PS (1970b) The use of backscattered electrons in high resolution scanning electron microscopy. Proc. 5th Nat. Conf. El. Probe Analysis 52A-52D.

Pawley JB (1974) Performance of SEM scintillation materials. Scanning Electron Microsc. 1974: 27-34.

Pawley JB (1984) Low voltage scanning electron microscopy. J. Microscopy 136:45-68.

Pawley JB (1988) The promise of Low Voltage SEM, Scanning 10:1.

Pawley JB, Scala WR (1986) Low voltage SEM update. Proc. EMSA 44th annual Meeting 654-657.

Peters KR (1982a) Conditions required for high quality high magnification images in secondary electron - I scanning electron microscopy. Scanning Electron Microsc. 1982; IV:1359-1372.

Peters KR (1982b) Generation, collection and properties of an SE-I enriched signal suitable for high resolution SEM on bulk specimens. Electron Beam Interactions With Solids. SEM Inc. AMF O'Hare, Chicago, IL. 363-372.

Peters KR (1985) Working at higher magnification in scanning electron microscopy with secondary and backscattered electrons on metal coated biological specimens and imaging macromolecular cell membrane structures. Scanning Electron Microsc. 1985; III:1519-1544.

Postek MT, Keery WJ, Larrabee RD (1988) The Relationship Between Accelerating Voltage Electron Detection Modes to Linewidth Measurement in an SEM. Scanning 10:10-18.

Reimer L (1973) Scanning electron microscopy: systems and applications. The Institute of Physics London, 120-125.

Reimer L, Pfefferkorn G (1977) Abbildung mit

Sekundär-, Rückstreuelektronen und Probenströmen. In: Rasterelektronenmikroskopie. Springer Berlin p.112.

Reimer L (1978) Scanning electron microscopy present state and trends. Scanning 1:3-16.

Reimer L (1979) Electron-specimen interactions. Scanning Electron Microsc. 1979;II:111-124.

Reimer L (1982) Electron signal and detector strategy. In: Electron Beam Interactions with Solids, Proc. 1st. Pfefferkorn Conference, SEM Inc., AMF O'Hare (Chicago), IL, pp. 299-310.

Reimer L, Lodding B (1984) Calculation and tabulation of Mott cross-sections for large-angle electron scattering. Scanning 6:128-151.

Reimer L, Riepenhausen M (1985) Detector Strategy for Secondary and Backscattered Electrons Using Multiple Detector Systems. Scanning 7:221-238.

Reimer L, Tollkamp C (1980) Measuring the backscattering coefficient and secondary electron yield inside a SEM. Scanning 3:35-39.

Reimer L, Tollkamp C (1982) Recording of topography by secondary electrons with a two-detector system. In: Electron Microscopy 1982 Vol.2 Deutsche Ges. für Elektronenmikroskopie Frankfurt 543-544.

Reimer L, Volbert B (1979) Detector system for backscattered electrons by conversion to secondary electrons. Scanning 4 238-248.

Reimer L, Volbert B (1980a) Separation of topographic and material contrast in scanning electron microscopy by different detector systems. Eur. Congr. EM 1980 Hague Proc. Vol 3 172-173.

Reimer L, Volbert B (1980b) New detector system for conversion of backscattered to secondary electrons. Inst. Phys. Cong. Ser. NO 52 London 1980 Chapter 1, 89-92.

Reimer L, Volbert B (1982) The origin and correction of SEM imaging artifacts arriving from the use of the difference signal of two detectors. Philips Electr. Opt. Bull. No 118.

Reimer L, Pöpper W, Bröcker W (1978) Experiments with a small solid angle detector for BSE. Scanning Electron Microsc. 1978; I:705-710.

Reimer L, Riepenhausen M, Schierjott M (1986) Signal of backscattered Electrons at edges and Surface Steps in Dependence on Surface Tilt and Take-off Direction. Scanning 8:164-175.

Reimer L, Riepenhausen M, Tollkamp C (1984) Detector strategy for improvement of image contrast analogous to light illumination. Scanning 6:155-167.

Reimer L, Volbert B, Bracker P (1979) STEM semiconductor for testing SEM quality parameters. Scanning 2:96-103.

Reimer L, Badde HG, Seidel H, Bühring W (1971) Orientierungsanisotropie des Rückstreukoeffizienten und der Sekundärelektronenausbeute von 10-100 keV-Elektronen. Z. angew. Phys. 31:145-151.

Robinson VNE (1974a) The origins of the secondary electron signal in scanning electron microscopy J. Phys. D7:2169-2173.

Robinson VNE (1974b) The construction and uses of an efficient backscattered electron detector for scanning electron microscopy. J. Phys. E7:650-652.

Robinson VNE (1975) Backscattered electron imaging. Scanning Electron Microsc. 1975:51-60.

Robinson VNE (1980) Imaging with backscattered electrons in a scanning electron microscope. Scanning 3:15-26.

Robinson VNE (1987a) Theory and applications of an efficient backscattered electron detector in scanning electron microscopy. BEDO 1987 20:83-88.

Robinson VNE (1987b) Materials characterization using the backscattered electron signal in scanning electron microscopy.Scanning Microscopy 1(1):107-117.

Robinson VNE, George EP (1976) Atomic number intensity profiles in the scanning electron microscope-gold and aluminium. J. Microscopy 107: 85-91.

Robinson VNE, George EP (1978) Electron scattering in the SEM. Scanning electron Microsc.1978; I:859-868.

Robinson VNE, Cutmore NG, Burdon RG (1984) Quantitative composition analysis using the backscattered electron signal in a scanning electron microscope. Scanning Electron Microsc. 1984; II: 483-492.

Schauer P, Autrata R (1979) Electro-optical properties of a scintillation detector in SEM. Journal de microscopie et de spectroscopie electroniques 4:633-650.

Schauer P, Autrata R, Kvapil Ji, Kvapil Jos (1985) Influence of single crystal yttrium aluminates surfaces on their cathodoluminescent properties. 7th Czechoslovak Conf. on Electronic and Vacuum Physics Bratislava 1985 (Ed. A Guldan Institute of Electrical Engineering CSAV Bratislava) Proc. Part 1 265-271.

Schmoranzer H, Grabe H, Schieve B (1975) Energy analysis of large angle keV electron scattering from solid targets. Appl. Phys. Lett. 26: 483-485.

Schur K, Blaschke R, Pfefferkorn G (1974) Improved conditions for backscattered electron SEM micrographs on polished sections using a modified scintillator detector. Scanning Electron Microsc. 1974:1003-1010.

Seidel H (1969) Rückstreukoeffizient von kompaktem Material In: Reimer L, Pfefferkorn G, Rasterelektronenmikroskopie. Springer Berlin 1977 p.38.

Seiler H (1968) Die physikalischen Aspekte der Sekundärelektronenemission für die Raster-Elektronen-Mikroskopie. BEDO 1968 1:27-52.

Seiler H (1983) Secondary electron emission in the scanning electron microscope. J. Appl. Phys. 54: R1-R18.

Shimizu R, Ikuta T, Murata K (1972) The Monte Carlo technique as applied to the fundamentals of EPMA and SEM. J. Appl. Phys. 43:4233-4249.

Stevenson YK (1977) Graphical method for the analysis of multicomponent experimental decay data. Int. Appl. Rad. Isotopes 28: 909-918.

Stewart ADG (1962) Investigation of the topography of ion bombarded surfaces with a scanning electron microscope. Electron Microscopy 1962 (Philadelphia) Academic Press New York. Vol 1 D12-D13.

Suganuma T (1985) Measurement of surface topography using SEM with two secondary electron detectors. J. Electron Microsc. 34:328-337.

Swift JA, Brown AC (1970) Transmission scanning electron microscopy of sectioned biological

materials. Scanning Electron Microsc. 1970: 113-120.

Takahashi R (1977) Backscattered SEM using CdS layer scintillator proposal of reflected SEM. Scanning Electron Microsc. 1977:71-78.

Takeda T, Mayata T, Muramatsu F, Tomiki T (1980) Fast decay u.v. phosphor - $YAlO_3$:Ce. J. Electrochem. Soc. 127:438-444.

Thirlwall JT, Comins NR (1981) Evaluation of a P-47 phosphor powder detector for backscattered electrons in SEM. EM Soc. Southern Africa Comp. Durban 1981 Proc. Vol 11 23-24.

Thümmel HV (1974) Durchgang von Elektronen und Betastrahlung durch Materialschichten. Akademie-Verlag Berlin GDR. Ch 9-11.

Venables JA, Bin-Jaya R (1977) Accurate microcrystallography using electron backscattering patterns. Phil. Mag. 35:1317-1332.

Venables JA, Harland CJ (1973) Electron backscattering patterns - a new technique for obtaining crystallographic information in the SEM. Phil. Mag. 27:1193-1200.

Venables JA, Griffits BW, Harland CJ, Ecker KH (1974) Some developments in SEM instrumentation. Rev. Physique Applique 9:419-425.

Venables JA, Harland CJ, Bin-Jaya R (1975) Crystallographic orientation determination in the SEM using EBSP's and channel plates. Developments in Electron Microscopy and Analysis 1975 p.101-104 Inst. of Physic London-Bristol 1976.

Volbert B, Reimer L (1980) Advantages of two opposite Everhart Thornley detectors in SEM. Scanning Electron Microsc. 1980; IV:1-10.

Walther P, Kříž S, Müller M, Ariano BH, Brodveck V, Ott P, Schweigreber ME (1984) Detection of protein A gold 15 nm marked surface antigens by backscattered electrons. Scanning Electron Microsc. 1984; III:1257-1266.

Watanabe S (1972) The scanning electron microscopic study of the lymph node. Acta Haem. Jap. 35:483-505.

Wells OC (1970) New contrast mechanism for SEM. Appl. Phys. Lett. 16:151-153.

Wells OC (1971) Low-loss image for surface scanning electron microscope. Appl. Phys. Lett. 19:232-235.

Wells OC (1972a) Low-loss image formation in the surface SEM. Seventh Nat. Conf. El. Probe Analysis EPASA San Francisco, CA. 16A-16C.

Wells OC (1972b) Explanation of the low-loss image in the SEM in terms of electron scattering theory. Scanning Electron Microsc. 1972:169-176.

Wells OC (1974) Scanning Electron Microscopy. Mc Graw - Hill Book Co New York Ch. 6.

Wells OC (1975) Measurements of low-loss electron emission from amorphous targets. Scanning Electron. Microsc. 1975;43-50, 132.

Wells OC (1977) Backscattered electron image (BSI) in the scanning electron microscope (SEM). Scanning Electron Microsc. 1977; I:747-771.

Wells OC (1978) Effect of collector position on type - 2 magnetic contrast in the SEM. Scanning Electron Microsc. 1978; I:293-298.

Wells OC (1979) Effects of Collector Take-off Angle and Energy Filtering on the BSE Image in the SEM. Scanning 2:199-216.

Wells OC (1980) Simplified model for an amorphous or single crystal solid target in the scanning electron microscope. In: Microbeam Analysis 1980 D B Wittry (Ed) San Francisco Press. pp 17-21.

Wells OC, Bremer CG (1970) Collector Turret for Scanning Electron Microscope. Rev. Sci. Instrum. 41:1034-1037.

Wells OC, Broers AN, Bremer CG (1973) Method for examining solid specimens with improved resolution in the scanning electron microscope. Appl. Phys. Lett. 23:353-355.

Wiggins JW (1978) The use of scintillation detectors in the STEM. Proc. Ninth Int. Congr. Electron Micr. Toronto 1978 Vol 1 78-79.

Wiggins JW, Zubin JA, Beer M (1979) High resolution scanning transmission electron microscope at John Hopkins. Rev. Sci. Instrum. 50:403-410.

Wolf ED, Everhart TE (1969) Annular diode detector for high angular resolution pseudo-Kikuchi patterns. Scanning Electron Microsc. 1969:41-44.

Wolf RJ, Joy DC, Tansley DW (1972) A Transmission stage for the scanning electron microscope. J. Phys. E: Sci. Instrum. 5:230-233.

Yamamoto T, Nishizawa H, Tsuno K (1976) Magnetic domain contrast in backscattered electron image obtained with a scanning electron microscope. Phil. Mag. 34:311-325.

Zeldes N, Tassa M (1979) Conversion of existing SEM components to form an efficient backscattered electron detector, and its forensic applications. Scanning Electron Microsc. 1979; II:155-158.

Discussion with Reviewers

F. Hasselbach: Most people use plastic scintillators in their Everhart-Thornley detectors. The light output of scintillators is usually given in % relative to Anthracene (e.g., Nuclear Enterprises plastic scintillator NE 102A has an output of about 40% compared to Anthracen for 10 keV electrons (H.-H. von Schmeling Z. Physik 160, 520-526 (1960)). What is the relative light output of e.g., NE 102A or another type of plastic scintillator compared to your YAG and YAP single crystals of the same shape, geometrical arrangement and reflective coating if used on the same light pipe with a photomultiplier with optimum photocathode for the emission spectrum of each scintillator.

Author: At present, the manufacturers of electron microscopes do not nearly use plastic scintillators in ET detectors. The reasons are limited lifetime and lower efficiency compared to anorganic powders and YAG, restricted use in ultrahigh vacuum, etc.

It is not simple to make a comparison of relative efficiencies of different scintillators, because the light output signal from a scintillator is influenced by optical parameters of the scintillator and light guide (index of refraction of scintillator and light guide, shape of scintillator, kind of surface treatment, use of reflecting, antireflecting and diffusion layers on the scintillator surface, etc.). For example, compared to NE 102A (index of refraction 1.5), YAG shows higher light losses owing to the high index of refraction (1.84). A light guide made of a material with a higher index of refraction (sapphire - 1.74) gives a better light transfer at the YAG - light guide boundary than a light guide of Perspex type (1.49). A powdered YAG single crystal scintillator gives a higher light output signal than the initial YAG single crystal scintillator. This is caused by optical effects.

We made a comparison of the light output

signal from YAG and YAP discs (ø 10 mm,d = 0.7 mm), NE 102A disc and NE 102A film on Perspex disc substrate of the same size under constant conditions, described for the case of PMT with S 20 photocathode, at an incident beam energy of 10 keV and a current density of 1.10^{-9} A.cm^{-2} . We used a Perspex light guide (PMMA, index of refraction 1.49) in the form of a cylinder of 10 mm diameter and 5 cm long. The scintillator was placed on the upper base of the cylinder. No cement was used.
The relative light output signal (S) recorded as the anode current of the PMT was normalized with respect to NE 102A ($S_{NE\ 102A}$= 1). Then S_{YAG} = 2.10, S_{YAP} = 2.30, S_{P47} = 2.15, $S_{NE\ 102A\ film\ on\ a\ substrate}$ = 1.30. These results are valid for the optical configuration used. When designing a new detector it is always necessary to take into account the respective correlations and to fit all parts of the detector to the optical optimum.

V.N.E. Robinson: In your section on "Detector Philosophy" you state that plastic scintillators degrade rapidly and quote Pawley (1974). Pawley's experiment refers to SE detection where the SE's attracted back to approximately 1 sq mm scintillator, giving a scintillator lifetime of approximately 10 hours. When used in a BSE detector, similar radiation is spread over some 2500 sq mm, giving plastic scintillators a lifetime of well over 10,000 hours before significant degradation i.e., many years. This lifetime outlasts many SEM's. Why do you consider it is "most important" to outlast this?
Author: Pawley used in his experiment (1974) a 1 cm^2 scintillator not a 1 mm^2 one. If the collected current i_C = 10^{-10} A, and the collected acceleration voltage V_C = 12.5 kV, then the dose rate is 2.25 MRad/h. For this dose rate Pawley observed a decrease in efficiency to 50 %/h. Earlier Odham et al. (J. Inst. Nuc. Eng. 12, 4-6 (1971)) obtained the same result for a dose rate of 1.5 MRad/h. It is true that if a hemispherical scintillator is used, SE's are incident on an area smaller than 1 cm^2, so that the evaluation of the dose rate can be loaded with an error. However, it can be judged from the courses of curves in Fig. 4 (Pawley 1974) that the areas of the flat and hemispherical scintillators on which SE's are incident will not differ substantially.

Figure A (below) shows the results of our measurements of a) block plastic scintillator, b) thin plastic layer, obtained under the following conditions: scintillator area 1 cm^2, electron current density 1.10^{-8} A.cm^{-2} , accelerating voltage of PE's incident upon the scintillator 20 kV. The radiation dose decreases especially with increasing scintillator area and with decreasing electron current.

The area of 2500 mm^2 you mention represents a scintillator with dimensions 50 x 50 mm or a concave hemisphere ("2 π detector") of 40 mm diameter. Such a big scintillator is not even used in the wide angle annular Robinson's detector. Besides, the BSE's do not load the scintillator area uniformly, but they hit certain localities on the surface in greater or smaller amounts depending on the energy and angular distribution of the electrons. The places hit by greater amounts of electrons degrade more quickly than the others.

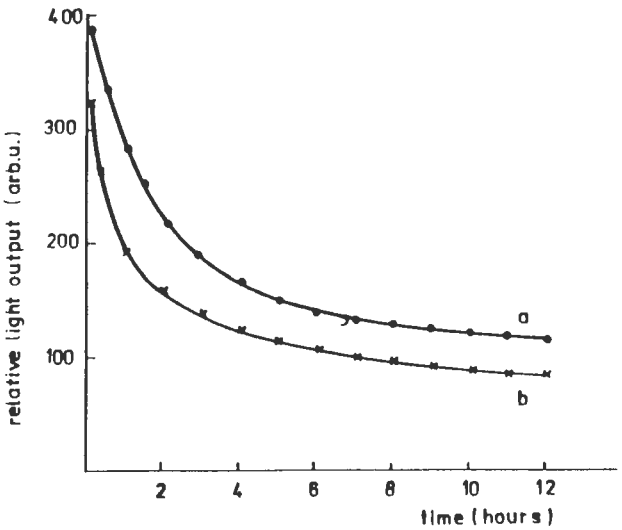

Figure A. Comparision of relative light output for block plastic scintillator (curve a) and thin plastic layer (curve b).

By our experience, it is possible to use a plastic scintillator in a BSE detector, but it is necessary to respect the value of the radiation dose which should not exceed 0.5 MRad. If a plastic scintillator is to be used for a long life operation in practice it is suitable to work with low current, sufficiently large scintillator area and, above all, lower electron energy.

P. Walther: In biology there is an increasing interest in working at low accelerating voltages (1 to 5 kV). Do you see a way to detect the BSE signal under these conditions?
Author: It is possible to detect the BSE signal at low accelerating voltages, 1 to 5 kV, of PE because the YAG scintillators coated with an extremely thin conducting layer of oxides of indium and tin are sensitive to incident electron energies from 1 keV. The signal obtained at an electron energy of 1 keV is, however, low and it is, therefore, more advantageous to accelerate the BSE's by a voltage of 3 to 5 kV applied to the conducting layer of the scintillator. The SE signal can be separated from the BSE signal so that the specimen is enclosed with an insulated grid and negative voltage is applied to the grid or a positive voltage is applied to the specimen.

V.N.E. Robinson: Your condition 1 for high resolution BSE imaging, high Z coating on low Z matrix is the same for high resolution SE imaging. Would you say that this supports Robinson's (1974) finding that most SE's are emitted by BSE's?
Author: We measured the yield of the individual components of the SE signal and found that the SE-I+II components amounted to 39 % for Au and 55 % for Al and the SE-III component to 43 % for Al and 58 % for Au of the total SE signal, which is in principle in accordance with the measurement results obtained by Peters (Scanning Electron Microsc. 1982, IV:1359-1372). The SE-III component represents thus nearly one half of the SE signal.

The subject of the inquiry is the yield of the SE-II component. Here, the situation is more complicated, because no accurate, perfect method for the separation of SE-II from SE-I has been developed yet. Murata (SEM/I, 267, 1973), Joy (J. Microsc. 136, 241, 1984), Reimer and Volbert (Scanning 4, 238, 1979) describe the yield of the SE-II component by the coefficient $\beta = 2 - 3$, Robinson (J. Phys. D7, 2169, 1974) gives $\beta_1 = 12 - 25$. From the condition 1 (in this paper) given for the high resolution of the BSE image it is difficult to judge which value of the yield of SE-II is more correct.

From our experiment of the determination of the mentioned condition of high resolution of the BSE image it is not possible to determine to what extent the SE-II component participates in the total SE signal. We were interested particularly in the SE-III signal representing BSE's. If the surface of a specimen with a low Z is covered with a thin layer with a high Z, then BSE's will emerge only from this thin layer, because the bulk material of the specimen under this thin layer has a very low coefficient of backscattering (according to its Z). When PE's pass through a thin layer with a high coefficient of backscattering, those BSE's emerge from the specimen which are generated in the vicinity or within the spot of PE's and not those which are diffusion scattered in the depth of the bulk specimen with a low coefficient of backscattering. The resulting image is dependent on the thickness of the thin layer with a high Z, energy of PE's, spot diameter of PE's and difference of coefficients of backscattering of both materials.

This condition is valid also for high resolution of an SE image, because the SE-II signal probably decreases in the specimen prepared as described above. It is difficult to say to what extent the SE-II signal decreases and how many SE's are then emitted by BSE's.

F. Hasselbach: Which types of photocathodes are the optimum to be used in connection with your two single crystal scintillators?
Author: The most advantageous for use in connection with YAG or YAP is a classical PMT with the S 20 photocathode. The S 11 photocathode which is used more frequently shows a 30% decrease in sensitivity for the YAG 560 nm operating wavelength. For the YAP 378 nm wavelength S 11 shows the same sensitivity as S 20. However, the best photocathodes are those with negative electron affinity.

F. Hasselbach: What is the spatial resolution for a YAG-screen e.g., for 20 keV electrons?
Author: According to the curve shown in Figure B (computed by the Monte Carlo method) the spatial resolution of an YAG screen for 20 keV electrons is about 2.3 micrometers. Preliminary experimental observations on a 0.5 mm thick YAG screen (polished on both sides) indicate that the actual resolution will be probably better than that calculated theoretically. More precise experiments have not yet been performed.

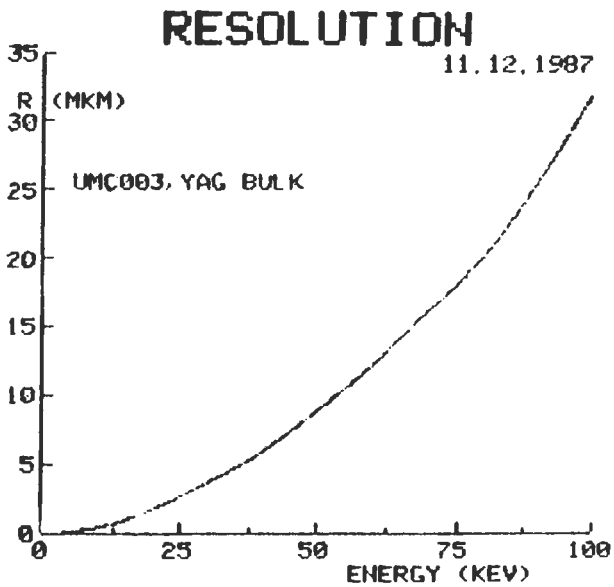

Figure B. Resolution curve for an YAG screen (courtsey of P. Schauer, Brno).

O. Johari: Please provide availability information on Autrata and Hejna (1989), Autrata and Mejzlik (1989), and several references from Proceedings where publisher information is not given.
Author: The pre-prints of first two references are available from me on request (see page 739). Regarding other references please note the following:

Proceedings of the 9th European Congress on Electron Microscopy, 1988 were published by the Institute of Physics, Bristol, U.K. Although several references state "Institute of Physics, London"; the Institute moved since the appearance of those papers and is now located in Bristol.

Proceedings of the 8th European Congress on Electron Microscopy, 1984 were published by Congress Bureau, P.O. Box 32, H-1361 Budapest, Hungary.

For BEDO series, please contact Prof. Ulrich Ehrenwerth, Buch/Zeitschriftenversand, Maringstr. 7, D-4400 Muenster, West Germany.

Regarding "Electron Microscopy 1978" Proceedings of the International Electron Microscopy Congress, contact: The Microscopical Society of Canada, Room 79, 150 College Street, Toronto, M5S 1A8.

Proceedings of the 10th Electron Microscopy International Congress, Hamburg, 1982 are available from Deutsche Gesellschaft fuer E.M., Am Roemerhof 35, D-6000 Frankfurt, West Germany.

Proceedings of the 6th European Electron Microscopy Congress were published by TAL International Publishing Co., Israel.

Proceedings of Electron Microprobe Analysis meetings are now available from San Francisco Press, San Francisco, CA.

For Proceedings of the annual EMSA meetings, information can be obtained from Dr. Morton Maser, P.O. Box EM, Woods Hole, MA 02543.

For the Thirlwall and Comins 1981 reference, contact the senior author directly: J.T. Thirlwall, C.S.I.R., Box 395, Pretoria 0001, South Africa.